Ctip1 Controls Acquisition of Sensory Area Identity and Establishment of Sensory Input Fields in the Developing Neocortex

Ctip1 controls acquisition of sensory area identity and establishment of sensory input fields in the developing neocortex

Luciano C. Greig[1,2,3], Mollie B. Woodworth[1,2,3], Chloé Greppi[1,2], and Jeffrey D. Macklis[1,2,*]

[1]Department of Stem Cell and Regenerative Biology, Center for Brain Science, and Harvard Stem Cell Institute, Harvard University, Cambridge, MA 02138, USA.
[2]Harvard Medical School, Boston, MA 02215, USA.
[3]These authors contributed equally to this work.
*Correspondence: jeffrey_macklis@harvard.edu

SUMMARY (147 words)

While several transcriptional controls over the size and relative position of cortical areas have been identified, less is known about regulators that direct acquisition of area-specific characteristics. Here, we report that the transcription factor *Ctip1* functions in primary sensory areas to repress motor and activate sensory gene expression programs, enabling establishment of sharp molecular boundaries defining functional areas. In *Ctip1* mutants, abnormal gene expression leads to aberrantly motorized corticocortical and corticofugal output connectivity. *Ctip1* critically regulates differentiation of layer IV neurons, and selective loss of *Ctip1* in cortex deprives thalamocortical axons of their receptive "sensory field" in layer IV, which normally provides a tangentially and radially defined compartment of dedicated synaptic territory. Therefore, although thalamocortical axons invade appropriate cortical regions, they are unable to organize into properly configured sensory maps. Together, these data identify *Ctip1* as a critical control over sensory area development.

RUNNING TITLE

Ctip1 directs acquisition of sensory area identity

HIGHLIGHTS

- Transcription factor *Ctip1* is highly expressed in all primary sensory areas.
- *Ctip1* directs acquisition of sensory area identity, and represses motor area identity.
- Output connectivity of sensory areas is partially motorized in *Ctip1* mutants.
- *Ctip1* establishes "sensory fields" in layer IV, enabling sensory map formation.

INTRODUCTION

The neocortex is responsible for processing and integrating all modalities of sensory information, generating precise motor output, and orchestrating higher-order cognitive tasks, a broad range of functions made possible by its tangential organization into specialized areas with distinct cytoarchitecture, connectivity, and patterns of gene expression (Rakic, 1988). In rodents, the neocortex is organized into four primary areas: motor (M1), somatosensory (S1), visual (V1), and auditory (A1). Area identity begins to be specified early in development by morphogens and signaling molecules secreted from patterning centers (Fukuchi-Shimogori and Grove, 2001; Toyoda et al., 2010; Garel et al., 2003; Assimacopoulos et al., 2012), which induce graded ventricular zone expression of several key transcription factors, including *Emx1/Emx2*, *Couptf1*, *Pax6*, *Sp8*, and *Tbr2* (O'Leary et al., 2007; Woodworth et al., 2012; Elsen et al., 2013). These regulators have been extensively studied, and appear to determine the final relative size and general position of cortical areas (Bishop et al., 2000; Hamasaki et al., 2004; Armentano et al., 2007; Piñon et al., 2008; Zembrzycki et al., 2013). Recent work has demonstrated that these early specification decisions are not made exclusively at the progenitor level, as had long been thought, and that postmitotic neurons, while partially programmed, are sufficiently plastic to fully change their area identity (Alfano et al., 2014).

Substantially less is known about molecular controls that drive differentiation of cortical neurons toward particular area identities, including expression of area-specific genes, extension of axonal projections to area-specific targets, and interactions with thalamocortical input that enable its organization into modality-specific topographic maps. The homeodomain transcription factor *Otx1* is required for areal refinement of subcerebral projection neuron connectivity (Weimann et al., 1999), but it remains unclear whether these changes in connectivity can be attributed to changes in molecular area identity. More recently, two transcription factors, *Bhlhb5* and *Lmo4*, have been shown to influence acquisition of molecular area identity (Joshi et al.,

2008; Sun et al., 2005). However, neither control is critical for establishment of cardinal features of area-specific connectivity, or for organization of sensory maps (Joshi et al., 2008; Ross et al., 2012; Sun et al., 2005; Huang et al., 2009; Cederquist et al., 2013). A third transcription factor, *Tbr1*, is expressed by postmitotic neurons and regulates early gene expression gradients, but *Tbr1* null mice die soon after birth, complicating investigation of later functions (Bedogni et al., 2010). Taken together, these studies begin to define molecular mechanisms directing area-specific differentiation in the cerebral cortex, but many important questions remain to be addressed.

Here, we identify that the transcription factor *Ctip1* acts postmitotically to regulate acquisition of sensory area identity, including the establishment of sensory-specific gene expression and output connectivity, as well as the organization of thalamocortical input into sensory maps. *Ctip1* was first described as an interacting partner of COUP transcription factors (COUP-TFs), which recruit *Ctip1* to potentiate transcriptional repression (Avram et al., 2000), but it can also regulate gene expression independently of COUP-TFs by binding specific DNA sequence motifs through its zinc finger domains (Avram et al., 2002; Xu et al., 2010). *Ctip1* has been most extensively studied in the hematopoietic system, where it controls specification of B-cells (Liu et al., 2003), and regulates the developmental switch from ɣ-globin to β-globin in red blood cells (Sankaran et al., 2008; Sankaran et al., 2009; Xu et al., 2011; Bauer et al., 2013). In the nervous system, *Ctip1* regulates dorsal interneuron morphogenesis and sensory circuit formation in the spinal cord (John et al., 2012), and *in vitro* studies also support a role in hippocampal neuron dendrite outgrowth and axon branching (Kuo et al., 2009; Kuo et al., 2010). More recently, *Ctip1* has been found to direct cortical projection neuron migration by regulating expression of Sema3c (Wiegreffe et al., 2015).

We report that *Ctip1* is also a critical postmitotic control over sensory area identity acquisition in the neocortex. Expression of CTIP1 in the cortical plate initially follows a high-caudomedial to low-rostrolateral gradient, and is refined further postnatally to be expressed

most highly in all primary sensory areas. In the absence of *Ctip1* function, there is a striking failure of molecular differentiation in primary sensory areas, as indicated by absent or reduced expression of sensory genes, and by ectopic expression of motor genes. These molecular abnormalities result in abnormal connectivity, with sensory callosal neurons aberrantly projecting to motor cortex in the contralateral hemisphere, sensory subcerebral neurons aberrantly maintaining projections to the spinal cord, and sensory corticothalamic neurons providing inappropriate input to motor thalamic nuclei. In addition, *Ctip1* regulates differentiation of layer IV neurons, and is, therefore, critical for the establishment of a receptive “sensory field" for thalamocortical input. Cortex-specific deletion of *Ctip1* deprives thalamocortical afferents of this dedicated synaptic territory, resulting in apoptosis of thalamocortical neurons in sensory thalamic nuclei, and severely disrupted organization of sensory maps in cortex. In an accompanying manuscript, we report that *Ctip1* functions as a critical control over projection neuron subtype specification in deep layers (Woodworth et al., submitted to Cell Reports), thereby linking sensory area identity acquisition to the generation of area-appropriate proportions of neuronal subtypes (Ramón y Cajal, 1899; Brodmann, 1909).

RESULTS

Ctip1 is highly expressed in primary sensory areas during development

CTIP1 can first be detected by immunocytochemistry in the cortical plate at approximately E12.5, and, by E15.5, it is also evident in the postmitotic migratory neurons of the intermediate zone (Figure 1A-1B and Woodworth et al., submitted to Cell Reports). Notably, expression of CTIP1 initially follows a high-caudomedial to low-rostrolateral gradient in both the intermediate zone and the cortical plate, with an approximately 1.5-fold difference in mRNA expression levels along both axes ($p<0.01$; Figure 1A-1B; Figure S1A-S1B). Over the course of development, CTIP1 expression undergoes progressive refinement to primary sensory areas. By P7, CTIP1 expression levels are quite low in motor cortex, and staining also becomes sparser across all layers, although areal differences between motor and sensory areas are most striking in layers VI, IV, and deeper II/III (Figure 1C-1D). In tangential sections through layer IV, CTIP1 distinctly labels primary somatosensory, visual, and auditory cortex (Figure 1E-1F).

The areal boundaries of CTIP1 expression almost exactly match those of BHLHB5, with strongest expression of both transcription factors in primary sensory areas (Figure S1E). At the cellular level, they are extensively co-expressed in layers II-V of somatosensory cortex, with 72±2% of BHLHB5-positive cells in superficial layers also expressing CTIP1 (Figure S1F-S1H). In contrast, the areal distribution of CTIP1 is complementary to that of LMO4, which is expressed in motor cortex and higher-order visual areas, but not in primary sensory areas (Figure S1I). Although there is more overlap between CTIP1 and LMO4 in layers V and VI of motor cortex, their expression is largely mutually exclusive in superficial layers, with only 25±4% of LMO4-positive cells expressing CTIP1 (Figure S1J-S1L).

Acquisition of sensory molecular area identity is disrupted in the absence of *Ctip1*

The initial gradient and progressive tangential refinement of CTIP1 expression motivated

us to investigate potential functions of *Ctip1* in acquisition of area identity. Because cortical arealization continues to unfold over the first week of postnatal development, and because *Ctip1*$^{-/-}$ mice die at birth (Liu et al., 2003), we pursued loss-of-function studies using *Ctip1*$^{fl/fl}$*;Emx1-Cre* cortex-specific conditional null mice, which survive to adulthood. As a first step toward interrogating area development in the absence of *Ctip1* function in these cortex-specific mutants, we performed ISH for several genes known to have areally-restricted expression patterns at P7, anticipating that reciprocal rostro-caudal shifts of motor- and sensory-specific gene expression would be indicative of complete respecification of area identity (O'Leary et al., 2007), while more complex disruptions would suggest abnormal acquisition of area identity (Joshi et al., 2008).

In *Ctip1*$^{fl/fl}$*;Emx1-Cre* brains, expression of several motor-specific genes expands into sensory areas, but sensory-specific genes do not undergo complementary caudal shifts, though they are expressed at severely reduced levels. For example, expression of axon guidance receptor *Epha7*, which is normally present in motor cortex and higher order visual areas, but excluded from somatosensory cortex (Figure 2A), expands to fill this "gap" (Figure 2B). Conversely, expression of the axon guidance cue *Efna5*, normally quite high in somatosensory cortex, is strikingly and specifically reduced (Figure 2C-2D). Expression of the cell adhesion molecule *Cdh6* expands caudally into higher order visual areas in layer II/III, while expression of the transcription factor *Id2* is lost in layer II/III in the same territory (Figure 2E-2H). Metabolic/cell-signaling enzyme *Cyp26b1* and transcription factor *Bhlhe40*, both of which are normally restricted to motor cortex, undergo striking caudal expansions in their expression domains (Figure 2I-2J, 2M-2N). In contrast, expression of cell adhesion molecule *Mdga1* and transcription factor *Cux1*, normally quite high in somatosensory cortex, is severely reduced, but does not appear to be shifted to more caudal positions (Figure 2K-2L, 2O-2P). Overall, there is a partial motorization of primary sensory areas, with motor-specific genes expanding caudally and sensory areas failing to express sensory-specific genes at appropriately high levels.

In order to monitor acquisition of molecular area identity globally throughout cortex, we performed wholemount β-galactosidase staining on brains carrying *LacZ* reporter alleles for either *Bhlhb5* or *Lmo4* (Feng et al., 2006; Deng et al., 2010). In wild-type mice, at P7, *Bhlhb5* is expressed only in primary sensory areas (Figure 2S), while *Lmo4* is highly expressed rostrally in motor cortex, medially in cingulate cortex, and caudally in higher-order visual areas, but is excluded from primary sensory areas, with sharp boundaries between these regions (Figure 2Q). Strikingly, in *Ctip1* conditional null mice, expression of *Bhlhb5* becomes faint and diffuse, such that primary somatosensory, visual, and auditory cortex can no longer be clearly discerned (Figure 2T). The boundary between somatosensory and motor cortex is still present, and its position is not shifted either rostrally or caudally. In contrast, expression of *Lmo4* in motor and cingulate cortex expands into somatosensory territory, such that the boundary between them shifts caudally (Figure 2R). Occipital *Lmo4* expression becomes compressed to a narrow band, such that primary visual cortex is no longer discernible. Importantly, establishment of molecular boundaries is comparatively preserved in the absence of either *Lmo4* or *Bhlhb5* function, using the same reporter alleles in *Lmo4*$^{fl/fl}$*;Emx1-Cre* and *Bhlhb5*$^{fl/fl}$*;Emx1-Cre* mice (Figure S2Q-S2V). Taken together, our data indicate that *Ctip1* acts after the initial positions of cortical areas have been at least partially established, and plays a critical role repressing motor identity and driving sensory differentiation.

To broaden our analysis and examine gene expression changes in *Ctip1*$^{fl/fl}$*;Emx1-Cre* mice using a high-throughput and unbiased approach, we performed RNA-seq on microdissected cortical areas. First, we compared gene expression between microdissected frontal (motor) and parietal (somatosensory) cortex in wild-type mice at P4, to prospectively identify genes that are more highly expressed in each area, and designated these differentially expressed transcripts M1 genes and S1 genes, respectively (Figure 2U; Table S1). We then compared gene expression between microdissected wild-type parietal cortex and *Ctip1*$^{fl/fl}$*;Emx1-Cre* parietal cortex, and specifically examined how loss of *Ctip1* function affects expression of

M1 genes and S1 genes (Figure 2V; Table S2). Of 329 M1 genes that are abnormally expressed in parietal cortex of *Ctip1* conditional nulls, 298 are upregulated and 31 are downregulated. Conversely, of 238 S1 genes that are abnormally expressed in parietal cortex of *Ctip1* conditional nulls, 210 are downregulated and 28 are upregulated. These data strongly reinforce the conclusion that *Ctip1* acts in somatosensory cortex to repress expression of motor genes and activate expression of sensory genes.

Having determined that *Ctip1* function is critical for acquisition of sensory area identity, we further investigated at which specific stages of development it functions. To rule out the possibility that, despite lack of expression in the proliferative zones, *Ctip1* might be necessary for early progenitor arealization, we investigated expression of *Pax6*, *Emx1*, *Emx2*, and *Couptf1*, and find that ventricular zone expression gradients of these early transcription factors are indistinguishable at E13.5 in wild-type and *Ctip1*$^{fl/fl}$*;Emx1-Cre* brains (Figure S2A-S2H), strongly indicating that progenitors are arealized independently of *Ctip1* function. However, by E17.5, "motor genes" such as *Lmo4* and *Bhlhe40* have already expanded into sensory territory (Figure S2I-S2J, S2M-S2N), concomitant with reduced expression of "sensory genes", such as *Mdga1* and *Odz3* (Figure S2K-S2L, S2O-S2P). These findings indicate that *Ctip1* regulates acquisition of sensory area identity by postmitotic neurons from early developmental stages.

Ctip1 functions cell-autonomously to establish sensory-area-specific callosal projection neuron connectivity

Callosal projection neurons (CPN) extend axons to mirror-image locations in corresponding cortical areas of the contralateral hemisphere, enabling highly organized inter-hemispheric transfer and integration of motor, somatosensory, visual, and auditory information (Yorke and Caviness, 1975; Richards et. al., 2004; Greig et al., 2013). Because *Ctip1* is highly expressed by CPN, and because CPN molecular area identity is severely disrupted in *Ctip1* mutants, we hypothesized that *Ctip1* might be important for establishment of areally precise

connectivity by sensory cortex CPN. To test this hypothesis, we performed two sets of experiments investigating the effects of both 1) global loss of *Ctip1* function throughout cortex and 2) cell-autonomous loss of *Ctip1* function in a small number of CPN.

In the first set of experiments, we focally injected adeno-associated virus expressing EGFP under a CMV/β-actin promoter (AAV-EGFP) into the cortices of *Ctip1*$^{fl/fl}$*;Emx1-Cre* and control mice. In wild-type mice, CPN axons from S1 innervate a narrow medio-lateral target area in the contralateral hemisphere, with two distinct clusters of innervation corresponding to the forelimb (S1FL) and upper lip (S1ULp) regions (Figure S3). In *Ctip1*$^{fl/fl}$*;Emx1-Cre* brains, CPN axons continue to project to approximately correct coordinates. However, the distinct clusters of innervation to S1FL and S1ULp are no longer discernible; rather, innervation becomes more uniform across the target field. This lack of precision in targeting might result from a corresponding lack of definition in the expression gradients of axon guidance molecules, such as *Epha7*, *Efna5*, and *Cdh6* (Figure 2A-2F).

Because any gradients of molecules controlling homotypic connectivity would change bilaterally and symmetrically in the absence of *Ctip1* function across the cortex, affecting both CPN and their contralateral projection targets, these bilateral changes might leave CPN targeting less sharply defined, but relatively intact, as we observed in the experiments described above. In the second set of experiments, therefore, we disrupted *Ctip1* expression unilaterally, to investigate whether this might create an areal mismatch between the two hemispheres, and result in more dramatically aberrant re-routing of CPN axons. We electroporated *Cre* and floxed(STOP)-*EGFP* expression constructs into the ventricular zone of *Ctip1*$^{fl/fl}$ and wild-type embryos at E14.5, when superficial-layer CPN are being generated, and collected brains with matched S1 electroporations at P7 (Figure 3A). In control experiments, *Cre*-electroporated wild-type neurons project almost exclusively homotypically to S1, with distinct clusters of innervation in S1FL and S1ULp, and little to no innervation of non-homotypic areas, including motor cortex more medially (M1/2), and secondary somatosensory (S2) and insular cortex (InsCx) more

laterally (Figure 3B). In striking contrast, *Cre*-electroporated *Ctip1*$^{fl/fl}$ neurons project across the entire medio-lateral extent of the contralateral hemisphere, without distinct clusters at S1FL and S1ULp (Figure 3C). Innervation of S1FL and S1ULp by S1 CPN lacking *Ctip1* is significantly reduced, and their axons are misrouted to M1/2 and InsCx ($p<0.05$ in each region; Figure 3D-3F). Taken together with our gene expression data, these results indicate that *Ctip1* is critical for proper areal specification of somatosensory cortex CPN, enabling precise targeting and refinement of connectivity between homotypic locations in the two cerebral hemispheres.

Ctip1 represses motor identity in sensory area corticothalamic projection neurons

The strong differential expression of CTIP1 between motor and sensory cortex in layer VI prompted us to investigate whether *Ctip1* might also direct acquisition of sensory area identity by corticothalamic projection neurons (CThPN), instructing them to establish connections with sensory thalamic nuclei. To anterogradely label CThPN axons, we injected AAV-*tdTomato* into M1, and AAV-*EGFP* into S1, of *Ctip1*$^{fl/fl}$*;Emx1-Cre* and wild-type pups at P1 (Figure 4A). We examined thalamic sections at P7 to determine whether motor and somatosensory CThPN innervated appropriate thalamic nuclei. In wild-type mice, motor CThPN project to the ventral lateral nucleus (VL), while somatosensory CThPN project to the ventral posterior nucleus (VP), with little overlap between the axons of these two populations (Figure 4B-4C). In *Ctip1*$^{fl/fl}$*;Emx1-Cre* mice, motor CThPN project normally to VA/VL (Figure 4D-4E), consistent with the lack of significant molecular abnormalities in motor cortex. In contrast, although a subset of somatosensory CThPN still project to VP in the absence of *Ctip1* function, many aberrantly innervate VL, leading to a striking increase in the overlap of somatosensory and motor cortical input in motor thalamus ($p<0.01$; Figure 4F), consistent with *Ctip1* functioning to repress motor identity in sensory areas. To directly investigate acquisition of molecular area identity by CThPN, we examined genes specifically expressed in either S1 or M1 of layer VI. We find that, in the absence of *Ctip1* function, there is a striking expansion in the expression of

motor-specific CThPN genes, such as *Crym* (Figure S4A-S4B), *Cyp26b1* (Figure S4C-S4D), and *Kitl* (Figure S4E-S4F), along with a reciprocal reduction in expression of sensory CThPN genes, such as *Mdga1* (Figure S4G-S4H). Taken together, these data indicate that *Ctip1* is required to repress motor identity in sensory CThPN.

In contrast, injection of AAV-EGFP and AAV-tdTomato into S1 and V1 (Figure 4G) reveals proper segregation of somatosensory and visual axons in both wild-type and *Ctip1*$^{fl/fl}$*;Emx1-Cre* brains, with somatosensory CThPN projecting to VP and visual CThPN projecting to the dorsolateral geniculate nucleus (Figure 4H-4K) and no significant difference in the overlap of somatosensory and visual input (Figure 4L). These results are consistent with the equivalently high levels of CTIP1 expression by CThPN in S1 and V1, which point toward a common function across all primary sensory areas. Expression of CTIP1 is necessary to prevent somatosensory CThPN from establishing connections with motor thalamic nuclei, but not for somatosensory and visual CThPN to establish connections with appropriate modality-specific sensory thalamic nuclei. Taken together, these data support the interpretation that *Ctip1* is specifically required for the broad distinction between CThPN specialized for motor output and those specialized for sensory output, but is not required for CThPN to become specialized for distinct sensory modalities.

Ctip1 represses motor identity in sensory area subcerebral projection neurons

Initially, subcerebral projection neurons (SCPN) in all areas of cortex send axons to the spinal cord, establishing collaterals to midbrain, pontine, and cerebellar nuclei along the way. This connectivity undergoes extensive pruning in the early postnatal period (P1-P21), such that SCPN in motor cortex maintain projections to the spinal cord and to the deep layers of the superior colliculus, while SCPN in visual cortex prune their projections to the spinal cord, and maintain projections to the superficial layers of the superior colliculus (Stanfield et al., 1982; Thong and Dreher, 1986). Interestingly, CTIP1 is progressively excluded from SCPN in motor

cortex (Woodworth et al., submitted to Cell Reports), but continues to be expressed at low levels by SCPN in somatosensory and visual cortex. At P4, only 6±2% of SCPN in motor cortex express CTIP1, while 73±3% of SCPN in sensory cortex express CTIP1 (Figure S4I-S4K).

To investigate the hypothesis that *Ctip1* might repress motor identity in sensory SCPN, we injected *AAV-tdTomato* into M1, and *AAV-EGFP* into V1, of wild-type and *Ctip1$^{fl/fl}$;Emx1-Cre* mice (Figure 4M). In wild-type mice, motor cortex SCPN project to the spinal cord and to the deep layers of the superior colliculus (Figure 4N-4R), and this precise area-specific connectivity is also evident in *Ctip1$^{fl/fl}$;Emx1-Cre* mice (Figure 4S-4W). Visual cortex SCPN rarely extend axons beyond the midbrain in wild-type mice (Figure 4P'-4Q'). In striking contrast, they aberrantly project into pons, through the medulla, and enter the dorsal corticospinal tract in *Ctip1$^{fl/fl}$;Emx1-Cre* mice (Figure 4U'-4V'). Moreover, instead of specifically targeting superficial layers, as they do in wild-type mice (Figure 4R'), visual cortex SCPN aberrantly innervate both superficial and deep layers of the superior colliculus in *Ctip1$^{fl/fl}$;Emx1-Cre* mice (Figure 4W'). We quantified this phenotype by retrogradely labeling from the dorsal corticospinal tract using Alexa Fluor 555-conjugated cholera toxin B (CTB-555) and counting the number of spinal cord-projecting neurons present in each cortical area at P21. Although approximately the same number of neurons in motor cortex maintain spinal projections in the absence of *Ctip1* function (Figure S4L-S4N), the number of neurons maintaining spinal projections increases approximately five-fold in somatosensory cortex ($p<0.05$), and approximately 20-fold in visual cortex ($p<0.01$; Figure S4O-S4T). These results from anterograde and retrograde labeling experiments clearly indicate that output connectivity of somatosensory and visual cortex SCPN becomes partially motorized in the absence of *Ctip1* function.

To examine whether SCPN in sensory cortex acquire a motor molecular identity in *Ctip1$^{fl/fl}$;Emx1-Cre* mice, we performed ISH for genes specifically expressed by SCPN in motor areas. In P7 wild-type brains, both *Igfbp4* and *Crim1* are strongly expressed by layer V neurons in motor areas, but are largely absent from layer V in sensory areas (Figure S4U, S4X).

Expression of *Igfbp4* and *Crim1* remains largely unchanged in M1 of *Ctip1*$^{fl/fl}$*;Emx1-Cre* mice (Figure S4V, S4Y). However, the expression domain of both genes expands dramatically into sensory areas, resulting in the number of neurons expressing *Igfbp4* increasing approximately three-fold in S1 and 24-fold in V1 ($p<0.01$; Figure S4W), and in the number of neurons expressing *Crim1* increasing approximately 15-fold in S1 and 30-fold in V1 ($p<0.01$; Figure S4Z). These data indicate that SCPN in sensory cortex become motorized in the absence of *Ctip1* function, and that this change in their transcriptionally specified area identity causes corresponding changes in connectivity.

Postnatal overexpression of *Ctip1* is sufficient to repress motor identity in subcerebral projection neurons

We next investigated whether *Ctip1* is sufficient to repress motor identity in postmitotic SCPN, performing gain-of-function *in utero* electroporation experiments. Because CAG-promoter-driven overexpression of *Ctip1* starting in progenitors drastically reduces the number of electroporated neurons that are specified as SCPN (Woodworth et al., submitted to Cell Reports), we used a tamoxifen-inducible form of *Cre* recombinase (*ER*^{T2}*-Cre-ER*^{T2}) to initiate expression of *EGFP* and/or *Ctip1* at P2, after subtype identity has already been established (Figure S5A-S5C). Highly efficient recombination upon tamoxifen induction was accomplished by using a FLEX-*FlpO* construct to couple relatively inefficient recombination by *ER*^{T2}*-Cre-ER*^{T2} with robust recombination of *frt-STOP-frt* cassettes by constitutively active *Flp* recombinase (Figure S5D-G). Expression constructs for *ER*^{T2}*-Cre-ER*^{T2} and FLEX-*FlpO*, together with conditional expression constructs for *EGFP* and/or *Ctip1*, were electroporated into the cortical ventricular zone at E12.5, and the resulting pups were injected with tamoxifen at P2 (Figure 5A-5C).

Using this strategy, we show that postnatal misexpression of *Ctip1* in motor cortex dramatically changes the pruning decisions of SCPN in this area, which normally do not express

Ctip1 during early postnatal development. Both *EGFP*-only and *EGFP*/*Ctip1* electroporations into motor cortex result in robust labeling of subcerebrally-projecting axons in the internal capsule at P21 (Figure 5D-5F, 5H-5J), with no significant difference between the two conditions (Figure 5L). However, while most EGFP-only electroporated SCPN maintain their spinal projections at P21 (Figure 5G), remarkably few *EGFP*/*Ctip1*-electroporated SCPN maintain their spinal projections at P21 (Figure 5K). This four-fold reduction in projections ($p<0.01$; Figure 5L) indicates that downregulation of *Ctip1* by SCPN in motor cortex during normal development is necessary to enable these neurons to maintain their spinal projections. Together, our loss- and gain-of-function data demonstrate that *Ctip1* represses motor identity in sensory area SCPN, instructing appropriate gene expression and final patterns of connectivity.

Thalamocortical input fails to organize into sensory maps in the absence of cortical *Ctip1* function

Given that sensory areas undergo striking motorization of output connectivity and gene expression in the absence of *Ctip1* function, we next examined whether organization of sensory thalamocortical input is also affected. Using serotonin (5HT) immunohistochemistry, we stained thalamocortical afferents, revealing sensory maps on tangential sections through layer IV of cortex. In wild-type brains, it is possible to discern, in sharp detail, the triangular visual map in occipital cortex, as well as the somatosensory "rodunculus" in parietal cortex, with its somatotopic representations of the hindlimb, forelimb, and lower jaw, and its field of vibrissal barrels, arranged precisely to reflect the positions of whiskers on the snout (Figure 6A). In *Ctip1*$^{fl/fl}$*;Emx1-Cre* mice, the entire sensory map is strikingly disorganized (Figure 6B). Blurry and imprecise representations of the hindlimb, forelimb, and lower jaw are still somewhat recognizable, but there are no similarly identifiable remnants of the triangular visual map, or the posteromedial barrel subfield. In spite of this severe disorganization, the overall size of the sensory and motor domains does not change (Figure 6C). Importantly, areal refinement of *Rorb*

and *Cdh8* expression, which depends on thalamocortical input (Chou et al., 2013; Vue et al., 2013), continues to reflect the overall configuration of sensory maps in *Ctip1$^{fl/fl}$;Emx1-Cre* mice (Figure S6A-S6E). These data demonstrate that cortex-specific deletion of *Ctip1* is sufficient to dramatically disrupt thalamocortical organization into sensory maps, but does not affect the relative size of the sensory and motor domains, or the ability of cortical neurons to modify their gene expression in response to signals from thalamocortical axons.

We next investigated the possibility that abnormal subplate development in *Ctip1$^{fl/fl}$;Emx1-Cre* mice might impair sensory map formation by disrupting navigation or topographic organization of thalamocortical axons *en route* to cortex, as successful invasion and preordering are both critical for subsequent map formation (Lopez-Bendito and Molnar, 2003; Lokmane et al., 2013). First, we examined the earliest stages of thalamocortical development by genetically labeling sensory thalamic nuclei in E14.5 wild-type and *Ctip1* null embryos by cross-breeding with *Gbx2-CreER^{T2}* and *Rosa26-floxed(STOP)-tdTomato* mice (Figure S6J). These anterograde labeling experiments demonstrate that thalamocortical axons project to cortex following a normal trajectory, and that a comparable number have reached the cortical plate at E14.5 in both wild-type and *Ctip1* null mice (Figure S6F-S6J). Next, we determined whether axons projecting to distinct regions of cortex in *Ctip1$^{fl/fl}$;Emx1-Cre* mice originate from neurons located in appropriate thalamic nuclei by injecting Alexa Fluor-conjugated CTB into frontal, parietal, and occipital cortex at P0, and then analyzing individual thalamic nuclei for retrograde labeling at P1. The overall organization of thalamocortical axons remains remarkably normal in *Ctip1$^{fl/fl}$;Emx1-Cre* mice, with clear labeling of VL/VA from frontal cortex, of VP from parietal cortex, and of dLG from occipital cortex (Figure S6M-S6T). Moreover, there is no significant difference in the proportion of input originating from each thalamic nucleus that innervates frontal, parietal, or occipital cortex (Figure S6U-S6V). We also directly visualized thalamocortical input at P1 on flattened cortices using 5HT immunohistochemistry. In wild-type mice, diffuse staining roughly delineates presumptive V1, A1, and S1 (Figure S6K). Although organization of

thalamocortical input is already less defined in *Ctip1*$^{fl/fl}$*;Emx1-Cre* brains at P1, the boundary between the motor and sensory domains is nonetheless clearly defined (Figure S6L). These data indicate that thalamocortical axons successfully reach appropriate regions of cortex in the absence of cortical *Ctip1* function, but are subsequently unable to refine into topographically-organized sensory maps.

To address the possibility that *Ctip1* function in *Emx1*-expressing cells outside the cerebral cortex might cause or contribute to this phenotype, we investigated formation of sensory maps in the brainstem and thalamus, using cytochrome oxidase staining to reveal the somatotopic representation of whiskers in the spinal trigeminal nucleus of the medulla (barrelettes) and in the VP of thalamus (barreloids). Importantly, we find that barrelettes in the spinal trigeminal nucleus are just as distinct and precisely arranged in *Ctip1*$^{fl/fl}$*;Emx1-Cre* brains as they are in wild-type controls (Figure 6D-6F). In thalamus, individual barreloids are still present and organized into distinct rows in *Ctip1*$^{fl/fl}$*;Emx1-Cre* brains, but the entire VP is smaller, making fine details more difficult to discern (Figure 6G-6I). This regression of barreloids in thalamus is suggestive of sensory map remodeling via top-down plasticity, with apoptosis of thalamocortical neurons, as has recently been reported in *Pax6*$^{fl/fl}$*;Emx1-Cre* mice (Zembrzycki et al., 2013). To further investigate the possibility that loss of *Ctip1* in cortex might result in atrophy of sensory thalamic nuclei postnatally, we performed ISH for the serotonin transporter (*Sert*). Both VP and dLG are approximately normal in size in *Ctip1*$^{fl/fl}$*;Emx1-Cre* brains at P0, but shrink approximately 40% by P7 (Figure 6J-6N; $p<0.01$). This regression of VP and dLG is directly linked to apoptotic death of thalamocortical neurons, as we identify a three-fold increase in the number of cleaved caspase-3-positive apoptotic cells in thalamus at P3 (Figure 6O-6S). Importantly, there is no atrophy or increased apoptosis in motor thalamic nuclei such as VA/VL (data not shown). Taken together, these data indicate that, despite reaching appropriate cortical areas, sensory thalamocortical axons are unable to organize into topographic maps in the absence of cortical *Ctip1* function, and apoptosis of sensory thalamocortical neurons increases

substantially.

Ctip1 regulates differentiation of layer IV neurons, and is necessary for their proper integration into barrels

Thalamocortical axons invading the cortical plate interact extensively with layer IV neurons as they organize into precise topographic representations within a permissive sensory cortical field established under precise regulation by cortex-intrinsic transcriptional programs. We hypothesized that sensory maps might fail to form in *Ctip1$^{fl/fl}$;Emx1-Cre* mice due to abnormal development of this permissive sensory field more broadly, and of layer IV neurons in particular. Supporting this interpretation, nearly all *Scnn1a-Cre*-expressing layer IV neurons express *Ctip1* (83±3%; Figure S7A-S7C). In the absence of *Ctip1* function, cytoarchitectural organization of layer IV neurons in barrel cortex is entirely lost, whether examined by DAPI staining (Figure 7A-7B) or by expression of *Rorb* (Figure 7C-7D). Although layer IV remains readily identifiable by *Rorb* expression in coronal sections (Figure 7E, 7I), we find strikingly reduced or entirely absent expression of other layer IV-specific genes, including the cell adhesion molecule *Mdga1* (Figure 7F, 7J), the metabotropic glutamate receptor *Grm4* (Figure 7G, 7K), and the transcription factor *Dbp* (Figure 7H, 7L). Concomitantly, there is markedly increased expression of several genes that are normally excluded from layer IV, including axonal outgrowth regulator *Gap43* (Figure S7D, S7G), transcription factor *Nex1* (Figure S7E, S7H), and intracellular sorting receptor *Sorl1* (Figure S7F, S7I). To investigate whether these molecular abnormalities affect compartmentalization of input within cortex, we combined 5HT immunostaining, to label thalamocortical input, with contralateral injection of AAV-EGFP, to label callosal input (Figure 7M). In wild-type mice, thalamocortical input clusters into distinct barrels, while callosal input from contralateral S1 is clearly excluded from the barrel compartment (Figure 7N-7O; quantified in 7R). In *Ctip1$^{fl/fl}$;Emx1-Cre* mice, thalamocortical input is still restricted to layer IV, though barrels are absent and staining is markedly reduced; even more

strikingly, there is robust callosal input to layer IV (Figure 7P-7Q; quantified in 7R). These data indicate that *Ctip1* regulates expression of layer IV-specific genes, and is required for layer IV neurons to receive specific sensory thalamocortical input and to successfully establish the appropriate cytoarchitectural organization to receive this input.

To gain further insight into the abnormal development of layer IV neurons in *Ctip1$^{fl/fl}$;Emx1-Cre* mice, we investigated the effects of cell-autonomous loss of *Ctip1* function. For these experiments, *CAG-Cre* and *CAG-floxed(STOP)-EGFP* expression constructs were electroporated into somatosensory cortex of *Ctip1$^{fl/fl}$* embryos or wild-type controls at E14.5 to target layer IV neurons. ROR-β immunostaining was performed on tangential sections through layer IV in order to evaluate the distribution of electroporated neurons within the barrel field (Figure 7S). *Cre*-electroporated neurons in wild-type brains adopt an unbiased distribution, so that more electroporated neurons are present in barrel walls, where cell density is higher (Figure 7T). Remarkably, *Cre*-electroporated neurons in *Ctip1$^{fl/fl}$* brains completely avoid barrels, and instead position themselves exclusively between barrels, within the septae (Figure 7U). In addition, while most wild-type layer IV neurons orient their dendrites toward the center of each barrel to synapse with thalamocortical axons (Figure 7W; quantified in 7V), the dendritic trees of *Ctip1* null neurons accumulate in septae, completely avoiding barrels (Figure 7X; quantified in 7V). Electroporations were also performed at E13.5 to evaluate radial positioning of electroporated neurons across layers (Figure S7Q). Although these electroporations were not timed to predominantly target layer IV, *Cre*-electroporated neurons in wild-type brains are nonetheless found at high density in layer IV, coinciding with ROR-β immunostaining (Figure S7O; quantified in S7Q). In contrast, *Cre*-electroporated neurons in *Ctip1$^{fl/fl}$* brains are primarily found deep or superficial to layer IV, and the few neurons in layer IV reside primarily between barrels, within the septae (Figure S7P; quantified in S7Q). Importantly, mosaic loss of *Ctip1* function in a subset of layer IV neurons does not interfere with the ability of thalamocortical axons to organize into properly configured sensory maps (Figure S7J-S7N). These experiments

indicate that *Ctip1* function is necessary for the integration of layer IV neurons into barrels, and for their assembly into the circuits that receive sensory information from thalamocortical afferents.

Ctip1 functions in layer IV to establish a permissive cortical field for sensory map formation

To determine whether *Ctip1* acts directly downstream of transcriptional programs that promote specification of sensory area identity, we investigated its genetic interactions with *Couptf1* (Armentano et al., 2007; Alfano et al. 2014). Most CTIP1-positive neurons in sensory areas also express COUPTF1 (Figure S8A-S8E; 71±4%), suggesting that *Couptf1*, which is expressed earlier in development, might activate expression of *Ctip1*. To test this hypothesis, we analyzed CTIP1 immunostaining in *Couptf1$^{fl/fl}$;Emx1-Cre* mice, and find that it is reduced in areas that have been respecified to acquire motor identity, but preserved in the caudally displaced sensory domain (Figure S8F-S8G). These data indicate that *Ctip1* expression is responsive to changes in area identity specification, but turns on within the sensory domain independently of *Couptf1* function. Conversely, in *Ctip1$^{fl/fl}$;Emx1-Cre* mice, COUPTF1 expression is clearly preserved, though at somewhat reduced levels (Figure S8H-S8I). These data indicate that regulation of sensory area identity acquisition by *Ctip1* increases *Couptf1* expression levels.

Since neither transcription factor is required for expression of the other, we investigated their epistatic relationship by generating double conditional null mice (*Ctip1$^{fl/fl}$;Couptf1$^{fl/fl}$;Emx1-Cre*). We focused on sensory map formation, because the single conditional mutants have largely non-overlapping phenotypes, with caudal displacement of thalamocortical input in *Couptf1$^{fl/fl}$;Emx1-Cre* mice (Figure 8B, 8F, 8G; Armentano et al., 2007; Alfano et al. 2014), but not in *Ctip1$^{fl/fl}$;Emx1-Cre* mice (Figure 6B), and a dramatic failure in organization of topographic maps in *Ctip1$^{fl/fl}$;Emx1-Cre* mice, but not in *Couptf1$^{fl/fl}$;Emx1-Cre* mice. Interestingly, combined

loss of cortical *Ctip1* and *Couptf1* function results in a largely additive phenotype, with thalamocortical input both caudally displaced and unable to organize into topographic maps (Figure 8C, 8H, 8I). Taken together, these data suggest that *Couptf1* and *Ctip1* have largely independent functions, with *Couptf1* determining the size and position of the sensory domain, and *Ctip1* regulating subsequent differentiation within that domain.

To investigate whether the requirement for *Ctip1* function in sensory map formation is primarily related to its function in layer IV neuron differentiation, we performed *in utero* electroporation surgeries to restore *Ctip1* expression exclusively in superficial layers of *Ctip1*$^{fl/fl}$*;Emx1-Cre* cortex (Figure 8J). In control *Egfp*-only experiments, thalamocortical afferents established substantially disorganized maps, with rudimentary somatotopic representations, but no recognizable barrel field, as expected (Figure 8K-8M). Remarkably, however, *Ctip1* expression in superficial layers was sufficient to rescue organization of thalamocortical afferents into precisely arranged rows of distinctly formed barrels in the most densely electroporated portion of somatosensory cortex (Figure 8N-8P). In combination with our earlier data on layer IV neuron differentiation, these experiments demonstrate that *Ctip1* acts cell-autonomously to establish a receptive field of dedicated synaptic territory in layer IV that enables thalamocortical afferents to organize into properly configured sensory maps.

DISCUSSION

Elucidating transcriptional programs that direct specialization of cortical areas is critical for understanding the emergence of area-specific connectivity, cytoarchitecture, and function, as well as the diversification of neuronal subtypes and their precise differentiation during cortical development. We report here that *Ctip1* is highly expressed in primary sensory areas, and that it is a critical control over acquisition of sensory molecular area identity (Figure 8Q). By repressing motor programs, *Ctip1* prevents projection neurons in sensory cortical areas from establishing

aberrant connections to motor-specific targets. In addition, *Ctip1* regulates differentiation of layer IV neurons and their integration into thalamorecepient circuits, which is critical, in turn, for organization of thalamocortical afferents into appropriately-configured topographic maps. Taken together, our findings indicate that *Ctip1* acts across multiple neuronal subtypes to coordinately regulate sensory-specific gene expression, thus linking output connectivity, cytoarchitectural organization, and sensory map formation during development.

Postmitotic controls intersectionally regulate acquisition of molecular area identity

Genes belonging to diverse functional categories are expressed in an area-specific fashion, including transcriptional regulators (*e.g.*, *Id2* and *Rorb*; Neuman et al., 1993; Nakagawa and O'Leary, 2003; Jabaudon et al., 2011), cell adhesion molecules (*e.g.*, *Cdh6* and *Cdh8*; Suzuki et al., 1997), intracellular signaling molecules (*e.g.*, *Plcb1*; Hannan et al., 2001), and axon guidance molecules (*e.g.*, *Epha7* and *Efna5*; Rubenstein et al., 1999; Dufour et al., 2003). Although they are useful readouts of area identity, the complex expression patterns of these genes represent the final outcome of intersectional regulation by multiple transcriptional programs acting in specific cortical layers and areas, rather than directly illuminating the basic organizational principles governing cortical arealization (Greig et al., 2013). The identification of transcriptional controls over postmitotic acquisition of area identity, such as *Bhlhb5*, *Lmo4*, and *Tbr1* (Joshi et al., 2008; Sun et al., 2005; Bedogni et al., 2010; Cederquist et al., 2013) will enable deconstructing this complex regulatory network into individual "developmental vectors" acting within defined tangential and laminar domains to intersectionally establish the more complex expression patterns of downstream genes.

We show here that *Ctip1* is critical for the establishment of molecular boundaries between motor and sensory areas, which are comparatively preserved in the absence of either *Lmo4* or *Bhlhb5* function (Figure S2). Broadly speaking, our RNA-seq data demonstrate that *Ctip1* acts within the sensory domain to repress expression of motor genes and to activate

expression of sensory genes (Figure 2U-2V). However, individual genes demonstrate complex patterns of misexpression in the absence of *Ctip1*. For example, *Lmo4* expands from motor and cingulate cortex into somatosensory territory, and recedes from higher-order visual areas into a narrow caudal band (Figure 2Q-2R). These symmetrically opposite changes suggest that *Lmo4* expression in motor and cingulate cortex might be established by mechanisms independent from those acting in higher-order visual areas, with *Ctip1* acting intersectionally with other regulators to activate or repress *Lmo4* expression, depending on context. Moreover, *Ctip1* functions in a number of distinct subtype-specific cellular contexts, potentially cooperating and competing with distinct sets of transcription factors in each neuronal subtype. Some of the changes in area-specific gene expression we have identified are consistent across subtypes (*e.g.*, *EphA7* and *EphrinA5*, Figure 2A-2D), while others affect one specific neuronal subtype, while spare other neuronal subtypes, (*e.g.*, *Cdh6* and *Id2*, Figure 2E-2H). These data suggest that *Ctip1* controls area identity both by regulating a common set of genes across multiple neuronal subtypes (acting autonomously or interacting with broadly expressed transcriptional regulators), and by regulating other sets of genes in a subtype-specific fashion (interacting with subtype-specific transcriptional regulators). As further regulators are identified, it will be important to investigate their functional interactions using both genetic and biochemical approaches.

Ctip1 **acts genetically downstream of** ***Couptf1,*** **and in parallel with** ***Bhlhb5***

We report here that *Ctip1* is positioned temporally and genetically downstream of *Couptf1*, which indirectly influences expression of *Ctip1* by regulating specification of sensory area identity (Figure S8F-S8G). However, *Couptf1* is not required for normal *Ctip1* expression within the sensory domain, suggesting that other progenitor-level controls are responsible for activating and directly regulating expression of *Ctip1*. Possible candidates are *Emx1* and *Emx2*, because their high-caudomedial to low-rostrolateral expression gradient in progenitors

(Gulisano et al., 1996) closely matches the early expression gradient of *Ctip1* in the cortical plate (Figure 1A-1B). The striking caudal shift in CTIP1 expression in *Couptf1* conditional nulls might result from the corresponding caudal shift of *Emx1/Emx2* expression in progenitors (Armentano et al., 2007). Most studies of cortical arealization to date have focused on either progenitor-level or postmitotic controls; however, regulatory mechanisms that transfer area identity from a given progenitor to its neuronal progeny as they exit the cell cycle remain comparatively unexplored.

Although the similar temporal and areal expression patterns of *Ctip1* and *Bhlhb5* suggest that they might act downstream of a common set of regulators (Figure S1E-S1H), the two transcription factors have largely non-overlapping functions. First, molecular abnormalities in *Bhlhb5* null mice are much more limited (Joshi et al., 2008; Figure S2Q-S2V), and do not indicate overall motorization of the sensory domain that we identify here in *Ctip1*$^{fl/fl}$*;Emx1-Cre* mice (Figure 2A-2T). Second, while most SCPN axons fail to reach the pyramidal decussation in *Bhlhb5* nulls (Joshi et al., 2008; Ross et al., 2012), loss of *Ctip1* function has the opposite effect, and more neurons project to the spinal cord (Figure S4L-S4T). These findings reinforce that *Bhlhb5* plays a broad role promoting SCPN axon outgrowth, especially in caudal motor cortex, while *Ctip1* instructs SCPN to acquire sensory area identity. One potentially shared function of *Bhlhb5* and *Ctip1* is barrel development, since cytoarchitectural organization in layer IV is disrupted in both *Bhlhb5* null and *Ctip1*$^{fl/fl}$*;Emx1-Cre* mice (Joshi et al., 2008; Figure 7A-7D). However, these abnormalities are considerably more severe in *Ctip1*$^{fl/fl}$*;Emx1-Cre* mice, with abnormal layer IV neuron differentiation also preventing thalamocortical axons from clustering into barrels (Figure 6A-6B). Overall, *Ctip1* regulates multiple critical aspects of postmitotic acquisition of sensory area identity independently of *Bhlhb5*, though both are involved in cytoarchitectural organization of layer IV.

Acquisition of area identity by subcerebral projection neurons

It has long been appreciated that area-specific connectivity of SCPN arises by stereotyped pruning of a common set of branches during the first three weeks of rodent postnatal development (Stanfield et al., 1982; Thong and Dreher, 1986; O'Leary, 1992). However, it remains unclear what combination of genetic programs and neuronal activity regulates axon pruning (Vanderhaeghen and Cheng, 2010). Although loss of either *Otx1* or *Ctip2* leads to defective pruning of spinal axons by visual cortex SCPN (Weimann et al., 1999; Arlotta et al., 2005), neither transcription factor is expressed with area specificity.

In contrast, *Ctip1* is expressed primarily by SCPN in sensory, but not motor, areas by P7 (Figure S4I-S4J), before the initial extension of corticospinal axons and brainstem collaterals is complete. SCPN in visual and somatosensory cortex of *Ctip1*$^{fl/fl}$*;Emx1-Cre* mice aberrantly maintain spinal projections and express genes characteristic of motor SCPN (Figure 4S-4W, Figure S4U-4Z). These changes in area-specific gene expression indicate that *Ctip1* is not merely necessary for pruning in a general sense, but, rather, specifically represses motor SCPN identity. In fact, ectopic expression of *Ctip1* in motor cortex SCPN during the early postnatal period is sufficient to reprogram their final pattern of output connectivity (Figure 5). These findings extend classic transplantation experiments showing that visual cortex SCPN can change their pruning properties if they are relocated to motor cortex early in development (Stanfield and O'Leary, 1985; O'Leary and Stanfield 1989), and indicate a prolonged period of plasticity in SCPN acquisition of area identity.

Cortex-intrinsic regulation of layer IV neuron differentiation and sensory map formation

We report here that *Ctip1* links earlier cortex-intrinsic regulators that specify area identity with later cortex-extrinsic signals that are required for refinement of area identity by directing differentiation of layer IV neurons within the sensory domain. Deletion of *Ctip1* from cortex results in a striking failure of sensory map formation, with no discernible organization of thalamocortical axons into barrels (Figure 7B). Layer IV neurons lack any cytoarchitectural

organization (Figure 7B) and fail to express layer IV-specific genes (Figure 7F-7L). In addition, axon terminals of contralateral callosal projection neurons invade layer IV of *Ctip1*$^{fl/fl}$*;Emx1-Cre* cortex, infringing on synaptic territory normally reserved for thalamocortical input (Figure 7P-7R). Cell-autonomous loss of *Ctip1* function in layer IV neurons completely disrupts their integration into barrels and assembly into thalamorecepient circuits (Figure 7S-7W). Taken together, these data indicate that *Ctip1* is a cortex-intrinsic control acting within the sensory domain to regulate layer IV neuron differentiation, enabling appropriate spatial organization of their dendritic trees and interactions with thalamocortical input, which are in turn critical for subsequent stages of sensory area development.

Multiple lines of investigation have identified that thalamocortical axons provide information required both for sensory map formation, and for parallel changes in layer IV neuron cytoarchitectural organization and molecular area identity during the final stages of cortical arealization (Wu et al., 2011; Li and Crair, 2011). In *barrelless* (*Adcy1* null) mice, thalamocortical axons and layer IV neurons fail to segregate into individual barrels (Van der Loos et. al., 1986; Abdel-Majid et al., 1998) due to the loss of adenylyl cyclase-dependent signals normally conveyed by thalamocortical axons (Iwasato et al., 2008). Genetically blocking neurotransmission at thalamocortical synapses disrupts barrel organization and molecular differentiation of layer IV neurons, which express severely reduced levels of *Dcdc2a* (Li et al., 2013). Additionally, genetic ablation of sensory thalamic nuclei disrupts refinement of gene expression, most prominently in layer IV, so that levels of *Rorb* and *Cdh8* become uniform throughout the sensory domain (Chou et al., 2013; Pouchelon et al., 2014). Together, these data highlight the importance of extrinsic signals for proper postnatal differentiation of cortical neurons.

Cortex-intrinsic programs acting at early stages of arealization have also been extensively investigated. Thalamocortical axons are attracted to specific regions of cortex by areally-specified cortical cues, which can be shifted rostrally or caudally by altering expression

of transcription factors specify area identity, like *Emx2* and *Couptf1* (O'Leary et al., 2007; Armentano et al., 2007). Once thalamocortical axons reach the cortical plate, however, their organization into sensory maps proceeds largely normally, regardless of the size or position of the respecified sensory domain (Hamasaki et al., 2004; Armentano et al., 2007; Zembrzycki et al., 2013). Importantly, loss of transcriptional controls over acquisition of sensory area identity has been associated with only subtle defects in cortical barrel cytoarchitecture and clustering of thalamocortical axons (Joshi et al., 2008). It has therefore remained unclear whether cortex-intrinsic programs direct differentiation of neurons within the sensory domain in order to enable the complex interactions with thalamocortical axons that are required for sensory map formation and further refinement of gene expression. We show here that *Ctip1* is a critical control over precisely this process in layer IV of sensory areas.

The complex interplay of cortex-intrinsic and cortex-extrinsic mechanisms in the specification of projection neuron area identity has important implications for a variety of neurodevelopmental disorders, but the precise molecular controls underlying these interactions remain poorly understood. Identification of *Ctip1* as a central regulator of layer IV neuron differentiation represents an important first step toward defining specific molecules that direct layer IV dendritic development, cytoarchitectural organization, and circuit integration. It will be of particular interest, in future studies, to investigate potential interactions between cortex-intrinsic transcription factors that control neuronal subtype and area identity, and transcription factors operating under the influence of thalamocortical activity. Further elucidation of the transcriptional mechanisms and molecular programs by which *Ctip1* regulates cortex-intrinsic aspects of arealization will offer important insights into the evolutionary and functional compartmentalization of cortex into distinct areas, and will also identify potential nodes of intersection with recently delineated maturational processes driven by thalamocortical input.

EXPERIMENTAL PROCEDURES

Animals

All mouse studies were approved by the Harvard University IACUC, and were performed in accordance with institutional and federal guidelines. The date of vaginal plug detection was designated E0.5, and the day of birth as P0. Unless noted otherwise, all experiments were performed using mice maintained on a C57BL6/J background, and *Ctip1*$^{fl/fl}$*;Emx1-Cre* experimental mice were controlled with *Ctip1*$^{wt/wt}$*;Emx1-Cre*.

Ctip1$^{fl/fl}$ mice were generated and generously shared by Tucker and colleagues (Sankaran et al., 2009). *Bhlhb5-LacZ*, *Lmo4-LacZ,* and *Lmo4*$^{fl/fl}$ mice were generated and generously shared by Gan and colleagues (Deng et al., 2010; Feng et al., 2006). *Couptf1*$^{fl/fl}$ mice were generated and generously shared by Studer and colleagues (Armentano et al., 2007; Tomassy et al., 2010). *Bhlhb5*$^{fl/fl}$ mice were generated by Greenberg and colleagues (Ross et al., 2012), and generously shared by Sarah Ross. *Emx1-Cre* mice were generated by Jones and colleagues (Gorski et al., 2002), and purchased from Jackson Laboratories (stock number 005628). *Scnn1a-Tg3-Cre* and *Rosa26-tdTomato-Ai9* mice were generated by Zeng and colleagues (Madisen et al., 2010), and purchased from Jackson Laboratories (stock numbers 009613 and 007909, respectively). *Gbx2-CreER*^{T2} mice were generated by Li and colleagues (Chen et al., 2009), and purchased from Jackson Laboratories (stock number 022135).

Immunocytochemistry, histology, and *in situ* hybridization

Mice were transcardially perfused with 4% paraformaldehyde, and brains were dissected and post-fixed at 4°C overnight. Tissue was sectioned at 50μm on a vibrating microtome (Leica). Embryonic brains were fixed at 4°C overnight, dissected, cryoprotected in 30% sucrose, and sectioned at 20μm on a cryostat (Leica). The following primary antibodies and dilutions

were used: rabbit anti-5HT, 1:20,000 (Immunostar); goat anti-BHLHB5, 1:300 (Santa Cruz); mouse anti-cleaved caspase 3, 1:500 (Abcam); rabbit anti-COUPTFI, 1:500 (gift from M. Studer), mouse anti-CTIP1 clone 14B5, 1:500 (Abcam); rabbit anti-GFP, 1:500 (Invitrogen); goat anti-LMO4, 1:200 (Santa Cruz); rabbit anti-RORB, 1:1000 (gift from H. Stunnenberg). Alexa Fluor-conjugated secondary antibodies (Invitrogen) were used at a dilution of 1:500. For 5HT immunohistochemistry, sections were developed using the Vectastain ABC kit. For cytochrome oxidase staining, 50μm vibratome sections were incubated at 37°C overnight in 0.1M phosphate buffer with 5% sucrose, 0.03% cytochrome *c*, and 0.05% DAB.

Riboprobe synthesis and nonradioactive *in situ* hybridization were performed using standard methods (Tiveron et al., 1996). Probe sources or primer sequences, as appropriate, are listed in Supplemental Experimental Procedures.

In utero electroporation

Surgeries were performed as previously described (Molyneaux et al., 2005). Briefly, plasmids were microinjected into the lateral ventricle of developing embryos under ultrasound guidance, and electroporated into cortical progenitors using a square wave electroporator (CUY21EDIT, Nepa Gene, Japan), set to deliver five 30V pulses of 50ms, separated by 950ms intervals. Tamoxifen induction was accomplished by intraperitoneal injection of 4OH-tamoxifen dissolved in corn oil (100ul at 5mg/ml; Sigma-Aldrich H6278 and C8267). Further details about plasmids used are provided in the Supplemental Experimental Procedures.

Anterograde labeling with AAV

All virus work was approved by the Harvard Committee on Microbiological Safety, and conducted according to institutional guidelines. Neurons were labeled by pressure injection of virus under ultrasound guidance into M1/S1 (Figure 4A-4E), S1/V1 (Figure 4G-4K), M1/V1 (Figure 4M-4W), or S1 (Figures S3A-S3B and 7M-7R) at P1, and brains were collected at P7.

For quantification, matched thalamic sections (Figure 4) or matched cortical sections (Figure S3 and 7) (n=3 mice for each genotype) were imaged, and fluorescence intensity was measured across images using ImageJ.

RNA sequencing

Frontal (motor) and parietal (somatosensory) cortex was dissected from P4 wild-type and *Ctip1*$^{fl/fl}$*;Emx1-Cre* mice, mRNA was isolated using mRNA Direct beads (Invitrogen), and libraries were prepared using NEBNext RNA Library Prep Kit (New England Biolabs). Sequencing was performed on an Illumina HiSeq 2500 at the Harvard Bauer core facility. Data was analyzed using Tuxedo tools (Trapnell et al., 2012).

AUTHOR CONTRIBUTIONS

L.C.G. and J.D.M. conceived the project; L.C.G. and M.B.W. designed and performed all experiments; L.C.G., M.B.W., and J.D.M. analyzed and interpreted the data; and L.C.G. and M.B.W. made figures. C.G. performed embryonic *in situ* hybridization experiments. L.C.G., M.B.W., and J.D.M. synthesized and integrated the findings, and wrote and revised the paper. All authors read and approved the final manuscript.

ACKNOWLEDGEMENTS

We thank L. Gan, E. Grove, S. Orkin, S. Ross, M. Studer, and H. Tucker for generous sharing of mice and reagents; B. Brandler, P. Davis, and E. Gillis-Buck for technical assistance; J. Flanagan, S. Dymecki, L. Goodrich, H. Padmanabhan, M.J. Galazo, and V. Sahni for scientific discussions; and members of the Macklis lab for helpful suggestions. This work was supported by grants to J.D.M. from the National Institutes of Health (NS045523, NS075672, and NS049553), with additional infrastructure support NS041590, the Harvard Stem Cell Institute, the Massachusetts Spinal Cord Injury Trust Fund, the Jane and Lee Seidman Fund for CNS Research, and the Emily and Robert Pearlstein Fund for Nervous System Repair. L.C.G. was partially supported by the Harvard Medical Scientist Training Program, NIH individual predoctoral National Research Service Award NS080343, and the DEARS Foundation. M.B.W. was partially supported by NIH individual predoctoral National Research Service Award NS064730 and the DEARS Foundation.

BIBLIOGRAPHY

Alfano, C., Magrinelli, E., Harb, K., Hevner, R.F., and Studer, M. (2014). Postmitotic control of sensory area specification during neocortical development. Nat Commun 5, 5632.

Arlotta, P., Molyneaux, B.J., Chen, J., Inoue, J., Kominami, R., and Macklis, J.D. (2005). Neuronal subtype-specific genes that control corticospinal motor neuron development in vivo. Neuron 45, 207–221.

Abdel-Majid, R.M., Leong, W.L., Schalkwyk, L.C., Smallman, D.S., Wong, S.T., Storm, D.R., Fine, A., Dobson, M.J., Guernsey, D.L., and Neumann, P.E. (1998). Loss of adenylyl cyclase I activity disrupts patterning of mouse somatosensory cortex. Nat Genet 19, 289–291.

Armentano, M., Chou, S.-J., Tomassy, G.S., Leingärtner, A., O'Leary, D.D.M., and Studer, M. (2007). COUP-TFI regulates the balance of cortical patterning between frontal/motor and sensory areas. Nat Neurosci 10, 1277–1286.

Assimacopoulos, S., Kao, T., Issa, N.P., and Grove, E.A. (2012). Fibroblast growth factor 8 organizes the neocortical area map and regulates sensory map topography. J Neurosci 32, 7191–7201.

Avram, D., Fields, A., Pretty On Top, K., Nevrivy, D.J., Ishmael, J.E., and Leid, M. (2000). Isolation of a novel family of C(2)H(2) zinc finger proteins implicated in transcriptional repression mediated by chicken ovalbumin upstream promoter transcription factor (COUP-TF) orphan nuclear receptors. J Biol Chem 275, 10315–10322.

Avram, D., Fields, A., Senawong, T., Topark-Ngarm, A., and Leid, M. (2002). COUP-TF (chicken ovalbumin upstream promoter transcription factor)-interacting protein 1 (CTIP1) is a sequence-specific DNA binding protein. Biochem J 368, 555–563.

Bauer, D.E., Kamran, S.C., Lessard, S., Xu, J., Fujiwara, Y., Lin, C., Shao, Z., Canver, M.C., Smith, E.C., Pinello, L., et al. (2013). An erythroid enhancer of BCL11A subject to genetic variation determines fetal hemoglobin level. Science 342, 253–257.

Bedogni, F., Hodge, R.D., Elsen, G.E., Nelson, B.R., Daza, R.A.M., Beyer, R.P., Bammler, T.K., Rubenstein, J.L.R., and Hevner, R.F. (2010). Tbr1 regulates regional and laminar identity of postmitotic neurons in developing neocortex. 107, 13129–13134.

Bishop, K.M., Goudreau, G., and O'Leary, D.D.M. (2000). Regulation of area identity in the mammalian neocortex by Emx2 and Pax6. Science 288, 344–349.

Brodmann, K. (1909 translated by Garey 2006). Brodmann's Localisation in the Cerebral Cortex (Springer Verlag).

Cederquist, G.Y., Azim, E., Shnider, S.J., Padmanabhan, H., and Macklis, J.D. (2013). Lmo4 Establishes Rostral Motor Cortex Projection Neuron Subtype Diversity. J Neurosci 33, 6321–6332.

Chou, S.J., Babot, Z., Leingärtner, A., Studer, M., Nakagawa, Y., and O'Leary, D.D.M. (2013). Geniculocortical Input Drives Genetic Distinctions Between Primary and Higher-Order Visual Areas. Science 340, 1239–1242.

Deng, M., Pan, L., Xie, X., and Gan, L. (2010). Requirement for Lmo4 in the vestibular morphogenesis of mouse inner ear. Dev Biol 338, 38–49.

Dufour, A., Seibt, J., Passante, L., Depaepe, V., Ciossek, T., Frisén, J., Kullander, K., Flanagan, J.G., Polleux, F., and Vanderhaeghen, P. (2003). Area specificity and topography of thalamocortical projections are controlled by ephrin/Eph genes. Neuron 39, 453–465.

Elsen, G. E., Hodge, R. D., Bedogni, F., Daza, R. A. M., Nelson, B. R., Shiba, N., et al. (2013). The protomap is propagated to cortical plate neurons through an Eomes-dependent intermediate map. Proceedings of the National Academy of Sciences of the United States of America, 110(10), 4081–4086.

Feng, L., Xie, X., Joshi, P.S., Yang, Z., Shibasaki, K., Chow, R.L., and Gan, L. (2006). Requirement for Bhlhb5 in the specification of amacrine and cone bipolar subtypes in mouse retina. Development 133, 4815–4825.

Fukuchi-Shimogori, T., and Grove, E.A. (2001). Neocortex patterning by the secreted signaling molecule FGF8. Science 294, 1071–1074.

Garel, S., Huffman, K.J., and Rubenstein, J.L.R. (2003). Molecular regionalization of the neocortex is disrupted in Fgf8 hypomorphic mutants. Development 130, 1903–1914.

Greig, L.C., Woodworth, M.B., Galazo, M.J., Padmanabhan, H., and Macklis, J.D. (2013). Molecular logic of neocortical projection neuron specification, development and diversity. Nat Rev Neurosci 14, 755–769.

Gorski, J.A., Talley, T., Qiu, M., Puelles, L., Rubenstein, J.L.R., and Jones, K.R. (2002). Cortical excitatory neurons and glia, but not GABAergic neurons, are produced in the Emx1-expressing lineage. J Neurosci 22, 6309–6314.

Gulisano, M., Broccoli, V., Pardini, C., and Boncinelli, E. (1996). Emx1 and Emx2 show different patterns of expression during proliferation and differentiation of the developing cerebral cortex in the mouse. Eur J Neurosci 8, 1037–1050.

Hamasaki, T., Leingärtner, A., Ringstedt, T., and O'Leary, D.D.M. (2004). EMX2 regulates sizes and positioning of the primary sensory and motor areas in neocortex by direct specification of cortical progenitors. Neuron 43, 359–372.

Hannan, A.J., Blakemore, C., Katsnelson, A., Vitalis, T., Huber, K.M., Bear, M., Roder, J., Kim, D., Shin, H.S., and Kind, P.C. (2001). PLC-beta1, activated via mGluRs, mediates activity-dependent differentiation in cerebral cortex. Nat Neurosci 4, 282–288.

Huang, Z., Kawase-Koga, Y., Zhang, S., Visvader, J., Toth, M., Walsh, C.A., and Sun, T. (2009). Transcription factor Lmo4 defines the shape of functional areas in developing cortices

and regulates sensorimotor control. Dev Biol 327, 132–142.

Iwasato, T., Inan, M., Kanki, H., Erzurumlu, R.S., Itohara, S., and Crair, M.C. (2008). Cortical adenylyl cyclase 1 is required for thalamocortical synapse maturation and aspects of layer IV barrel development. J Neurosci 28, 5931–5943.

Jabaudon, D., Shnider, S.J., J Tischfield, D., J Galazo, M., and Macklis, J.D. (2011). ROR{beta} Induces Barrel-like Neuronal Clusters in the Developing Neocortex. Cereb Cortex.

John, A.A., Brylka, H.H., Wiegreffe, C.C., Simon, R.R., Liu, P., Jüttner, R.R., Crenshaw, E.B., Luyten, F.P.F., Jenkins, N.A., Copeland, N.G., et al. (2012). Bcl11a is required for neuronal morphogenesis and sensory circuit formation in dorsal spinal cord development. Development 139, 1831–1841.

Joshi, P.S., Molyneaux, B.J., Feng, L., Xie, X., Macklis, J.D., and Gan, L. (2008). Bhlhb5 regulates the postmitotic acquisition of area identities in layers II-V of the developing neocortex. Neuron 60, 258–272.

Kocsis, E., Trus, B.L., Steer, C.J., Bisher, M.E., and Steven, A.C. (1991). Image averaging of flexible fibrous macromolecules: the clathrin triskelion has an elastic proximal segment. J. Struct. Biol. 107, 6–14.

Kuo, T.-Y., and Hsueh, Y.-P. (2007). Expression of zinc finger transcription factor Bcl11A/Evi9/CTIP1 in rat brain. J Neurosci Res 85, 1628–1636.

Kuo, T., Hong, C., and Hsueh, Y. (2009). Bcl11A/CTIP1 regulates expression of DCC and MAP1b in control of axon branching and dendrite outgrowth. Mol Cell Neurosci.

Kuo, T.-Y., Chen, C.-Y., and Hsueh, Y.-P. (2010). Bcl11A/CTIP1 mediates the effect of the glutamate receptor on axon branching and dendrite outgrowth. J. Neurochem. 114, 1381–1392.

Leid, M., Ishmael, J.E., Avram, D., Shepherd, D.M., Fraulob, V., and Dollé, P. (2004). CTIP1 and CTIP2 are differentially expressed during mouse embryogenesis. Gene Expr Patterns 4, 733–739.

Li, H., Fertuzinhos, S., Mohns, E., Hnasko, T.S., Verhage, M., Edwards, R., Šestan, N., and Crair, M.C. (2013). Laminar and columnar development of barrel cortex relies on thalamocortical neurotransmission. Neuron 79, 970–986.

Li, H., and Crair, M.C. (2011). How do barrels form in somatosensory cortex? Ann. N. Y. Acad. Sci. 1225, 119–129.

Liu, P., Keller, J.R., Ortiz, M., Tessarollo, L., Rachel, R.A., Nakamura, T., Jenkins, N.A., and Copeland, N.G. (2003). Bcl11a is essential for normal lymphoid development. Nat Immunol 4, 525–532.

Lokmane, L., Proville, R., Narboux-Nême, N., Györy, I., Keita, M., Mailhes, C., Léna, C., Gaspar, P., Grosschedl, R., and Garel, S. (2013). Sensory map transfer to the neocortex relies

on pretarget ordering of thalamic axons. Curr Biol 23, 810–816.

López-Bendito, G., and Molnár, Z. (2003). Thalamocortical development: how are we going to get there? Nat Rev Neurosci 4, 276–289.

Molyneaux, B.J., Arlotta, P., Hirata, T., Hibi, M., and Macklis, J.D. (2005). Fezl is required for the birth and specification of corticospinal motor neurons. Neuron 47, 817–831.

Nakagawa, Y., and O'Leary, D.D.M. (2003). Dynamic patterned expression of orphan nuclear receptor genes RORalpha and RORbeta in developing mouse forebrain. Dev Neurosci 25, 234–244.

Neuman, T., Keen, A., Zuber, M.X., Kristjansson, G.I., Gruss, P., and Nornes, H.O. (1993). Neuronal expression of regulatory helix-loop-helix factor Id2 gene in mouse. Dev Biol 160, 186–195.

O'Leary, D.D. (1992). Development of connectional diversity and specificity in the mammalian brain by the pruning of collateral projections. Curr Opin Neurobiol 2, 70–77.

O'Leary, D.D.M., and Stanfield, B.B. (1989). Selective elimination of axons extended by developing cortical neurons is dependent on regional locale: experiments utilizing fetal cortical transplants. J Neurosci 9, 2230–2246.

O'Leary, D.D.M., Chou, S.-J., and Sahara, S. (2007). Area patterning of the mammalian cortex. Neuron 56, 252–269.

Piñon, M.C., Tuoc, T.C., Ashery-Padan, R.R., Molnár, Z., and Stoykova, A. (2008). Altered molecular regionalization and normal thalamocortical connections in cortex-specific Pax6 knock-out mice. J Neurosci 28, 8724–8734.

Pouchelon, G., Gambino, F., Bellone, C., Telley, L., Vitali, I., Lüscher, C., Holtmaat, A., and Jabaudon, D. (2014). Modality-specific thalamocortical inputs instruct the identity of postsynaptic L4 neurons. Nature 511, 471–474.

Rakic, P. (1988). Specification of cerebral cortical areas. Science, 241(4862), 170–176.

Ramón y Cajal, S. (1899) Comparative Study of the Sensory Areas of the Human Cortex.

Richards, L.J., Plachez, C., and Ren, T. (2004). Mechanisms regulating the development of the corpus callosum and its agenesis in mouse and human. Clin Genet 66, 276–289.

Ross, S.E., McCord, A.E., Jung, C., Atan, D., Mok, S.I., Hemberg, M., Kim, T.-K., Salogiannis, J., Hu, L., Cohen, S., et al. (2012). Bhlhb5 and Prdm8 form a repressor complex involved in neuronal circuit assembly. Neuron 73, 292–303.

Rubenstein, J.L., Anderson, S., Shi, L., Miyashita-Lin, E., Bulfone, A., and Hevner, R. (1999). Genetic control of cortical regionalization and connectivity. Cereb Cortex 9, 524–532.

Sankaran, V.G., Menne, T.F., Xu, J., Akie, T.E., Lettre, G., Van Handel, B., Mikkola, H.K.A.,

Hirschhorn, J.N., Cantor, A.B., and Orkin, S.H. (2008). Human fetal hemoglobin expression is regulated by the developmental stage-specific repressor BCL11A. Science 322, 1839–1842.

Sankaran, V.G., Xu, J., Ragoczy, T., Ippolito, G.C., Walkley, C.R., Maika, S.D., Fujiwara, Y., Ito, M., Groudine, M., Bender, M.A., et al. (2009). Developmental and species-divergent globin switching are driven by BCL11A. Nature 460, 1093–1097.

Stanfield, B. B., O'Leary, D. D. M., and Fricks, C. (1982). Selective collateral elimination in early postnatal development restricts cortical distribution of rat pyramidal tract axons. Nature 298, 371-373.

Stanfield, B.B., and O'Leary, D.D.M. (1985). Fetal occipital cortical neurones transplanted to the rostral cortex can extend and maintain a pyramidal tract axon. Nature 313, 135–137.

Sun, T., Patoine, C., Abu-Khalil, A., Visvader, J., Sum, E., Cherry, T.J., Orkin, S.H., Geschwind, D.H., and Walsh, C.A. (2005). Early asymmetry of gene transcription in embryonic human left and right cerebral cortex. Science 308, 1794–1798.

Suzuki, S.C., Inoue, T., Kimura, Y., Tanaka, T., and Takeichi, M. (1997). Neuronal circuits are subdivided by differential expression of type-II classic cadherins in postnatal mouse brains. Mol Cell Neurosci 9, 433–447.

Thong, I, C., and Dreher, B. (1986). The development of the corticotectal pathway in the albino rat. Dev. Brain Res. 25, 227-238.

Toyoda, R., Assimacopoulos, S., Wilcoxon, J., Taylor, A., Feldman, P., Suzuki-Hirano, A., Shimogori, T., and Grove, E.A. (2010). FGF8 acts as a classic diffusible morphogen to pattern the neocortex. Development 137, 3439–3448.

Van der Loos, H., Welker, E., Dörfl, J., and Rumo, G. (1986). Selective breeding for variations in patterns of mystacial vibrissae of mice. Bilaterally symmetrical strains derived from ICR stock. J. Hered. 77, 66–82.

Vanderhaeghen, P., and Cheng, H.-J. (2010). Guidance molecules in axon pruning and cell death. Cold Spring Harb Perspect Biol 2, a001859.

Vue, T.Y., Lee, M., Tan, Y.E., Werkhoven, Z., Wang, L., and Nakagawa, Y. (2013). Thalamic control of neocortical area formation in mice. J Neurosci 33, 8442–8453.

Weimann, J.M., Zhang, Y.A., Levin, M.E., Devine, W.P., Brûlet, P., and McConnell, S.K. (1999). Cortical neurons require Otx1 for the refinement of exuberant axonal projections to subcortical targets. Neuron 24, 819–831.

Wiegreffe, C., Simon, R., Peschkes, K., Kling, C., Strehle, M., Cheng, J., Srivatsa, S., Liu, P., Jenkins, N.A., Copeland, N.G., Tarabykin, V., Britsch, S., 2015. Bcl11a (Ctip1) Controls Migration of Cortical Projection Neurons through Regulation of Sema3c. Neuron 87, 311–325.

Woodworth, M.B., Custo Greig, L., Ippolito, G.C., Tucker, H.O., and Macklis, J.D. (2013). Ctip1

regulates the balance between specification of distinct projection neuron subtypes in deep cortical layers. Submitted to Cell Reports.

Woodworth, M.B., Custo Greig, L.F., Kriegstein, A.R., and Macklis, J.D. (2012). SnapShot: Cortical Development. Cell 151, 918–918.e1.

Wu, C.-S., Ballester Rosado, C.J., and Lu, H.-C. (2011). What can we get from “barrels”: the rodent barrel cortex as a model for studying the establishment of neural circuits. Eur J Neurosci 34, 1663–1676.

Xu, J., Sankaran, V.G., Ni, M., Menne, T.F., Puram, R.V., Kim, W., and Orkin, S.H. (2010). Transcriptional silencing of {gamma}-globin by BCL11A involves long-range interactions and cooperation with SOX6. Genes Dev 24, 783–798.

Xu, J., Peng, C., Sankaran, V.G., Shao, Z., Esrick, E.B., Chong, B.G., Ippolito, G.C., Fujiwara, Y., Ebert, B.L., Tucker, P.W., et al. (2011). Correction of sickle cell disease in adult mice by interference with fetal hemoglobin silencing. Science 334, 993–996.

Yorke, C.H., Jr and Caviness, V.S., Jr (1975) Interhemispheric neocortical connections of the corpus callosum in the normal mouse: a study based on anterograde and retrograde methods. J. Comp. Neurol. 164, 233–245.

Zembrzycki, A., Chou, S.-J., Ashery-Padan, R.R., Stoykova, A., and O'Leary, D.D.M. (2013). Sensory cortex limits cortical maps and drives top-down plasticity in thalamocortical circuits. Nat Neurosci 16, 1060–1067.

FIGURE LEGENDS

Figure 1. Neocortical expression of CTIP1 becomes areally patterned as the neocortex matures.

(A-B) At E15.5, CTIP1 is expressed by newly postmitotic projection neurons in a low-rostrolateral to high-caudomedial gradient across the cortex. In coronal sections (A), CTIP1 is expressed by postmitotic projection neurons at higher levels medially (A') and lower levels laterally (A''), while in sagittal sections (B), CTIP1 is expressed at higher levels caudally (B') and lower levels rostrally (B'').

(C-F) By P7, CTIP1 is highly expressed in primary sensory areas. In coronal sections, a distinct boundary of CTIP1 expression exists between primary somatosensory and primary motor cortex (C), with sparser expression of CTIP1 in primary motor cortex (D') compared to primary sensory cortex (D''), especially in layer VI and deep layer II/III. In tangential sections of flattened cortex (E, F), CTIP1 expression clearly delineates primary sensory areas (V1, A1, and S1), and is absent from primary motor cortex (M1) and higher-order sensory areas.

A1, primary auditory cortex; M1, primary motor cortex; S1, primary somatosensory cortex; V1, primary visual cortex.

Scale bars: 500μm (D, F), 250μm (A, B), 25μm (A'-A'', B'-B'' and D'-D'')

Figure 2. Establishment of precise gene expression programs delineating motor and sensory areas is severely disrupted in *Ctip1*$^{fl/fl}$*;Emx1-Cre* cortex.

(A-P) In the absence of *Ctip1* function, molecular area identity in somatosensory cortex is severely disrupted. *EphA7*, largely excluded from wild-type somatosensory cortex (A), is extensively expressed in *Ctip1*$^{fl/fl}$*;Emx1-Cre* somatosensory cortex (B). The sharp caudal boundaries of wild-type *Efna5*, *Cdh6*, *Cyp26b1*, and *Bhlhe40* expression (C, E, I, M) are

replaced by gradual gradients that aberrantly invade occipital cortex in *Ctip1*$^{fl/fl}$*;Emx1-Cre* brains (D, F, J, N). Superficial-layer expression of *Id2* in wild-type somatosensory and visual cortex (G) is lost in *Ctip1*$^{fl/fl}$*;Emx1-Cre* cortex (H), while strong expression of *Mdga1* and *Cux1* in wild-type somatosensory cortex (K, O) is lost or greatly reduced in *Ctip1*$^{fl/fl}$*;Emx1-Cre* cortex (L, P).
(Q-T) Expression domains of *Bhlhb5* and *Lmo4* are strikingly abnormal in the absence of *Ctip1* function. At P7, when area identity refinement is normally complete, distinct primary and higher-order visual areas in wild-type cortex (Q) are not discernible in *Ctip1*$^{fl/fl}$*;Emx1-Cre* cortex (R) by *Lmo4*-driven *LacZ* expression. *Bhlhb5* expression is almost absent from *Ctip1*$^{fl/fl}$*;Emx1-Cre* cortex (T), compared with sharply-delineated sensory area expression in wild-type cortex (S).
(U-V) *Ctip1*$^{fl/fl}$*;Emx1-Cre* parietal cortex expresses genes characteristic of wild-type motor cortex, but not somatosensory cortex. We compared gene expression between wild-type frontal (M1) and parietal (S1) cortex at P4 by RNA-seq, designating genes enriched in one area as M1 or S1 genes, respectively (U). When wild-type and *Ctip1*$^{fl/fl}$*;Emx1-Cre* parietal cortex are compared, 298 of 329 differentially expressed M1 genes are increased in expression in *Ctip1* conditional mutants, and 210 of 238 differentially expressed S1 genes are decreased in expression (V).
A1, primary auditory cortex; M1, primary motor cortex; S1, primary somatosensory cortex; V1, primary visual cortex.
Scale bars: 500μm, all panels.

Figure 3. In the absence of *Ctip1* function, callosal projection neurons fail to project to homotypic locations in the contralateral hemisphere.
(A) Schematic of experimental approach. Embryos were electroporated at E14.5 with CAG-Cre and CAG-floxed(STOP)-EGFP plasmids, and brains were collected at P7. For quantification, images of electroporated and contralateral hemispheres of cortex were divided into 200 bins from the M1/S1FL boundary medially to the Ins. Ctx./Pir. Ctx. boundary laterally. Fluorescence

intensity was quantified in each bin using ImageJ.

(B-C) While axons of Cre-electroporated wild-type CPN cluster in S1FL and S1ULp (B), axons of Cre-electroporated *Ctip1*$^{fl/fl}$ CPN exhibit little areal specificity (C).

(D-F) Quantification of data in B-C. Although Cre electroporations into wild-type and *Ctip1*$^{fl/fl}$ brains were similar in size and location (D), axons of electroporated wild-type neurons clearly target specific areas of contralateral cortex preferentially, while axons of electroporated *Ctip1*$^{fl/fl}$ neurons distribute evenly across the medio-lateral extent of cortex (E). Significantly more axons from Cre-electroporated *Ctip1*$^{fl/fl}$ neurons aberrantly target motor cortex and insular cortex, and significantly fewer target forelimb and upper lip regions of primary somatosensory cortex (F). *, $p<0.05$.

(G-P) High magnification images of axons from B-C. Wild-type axons preferentially innervate S1FL and S1ULp (I, M), and avoid M1/M2, S1J, and Ins. Ctx. (G, K, O), while Cre-electorporated *Ctip1*$^{fl/fl}$ axons innervate all areas approximately equally (H, J, L, N, P).

M1, primary motor cortex; M2, secondary motor cortex; S1FL, primary somatosensory cortex, forelimb region; S1J, primary somatosensory cortex, jaw region; S1ULp, primary somatosensory cortex, upper lip region; S2, secondary somatosensory cortex; Ins. Ctx., insular cortex; Pir. Ctx., piriform cortex; CL, contralateral.

Scale bars: 100μm (B, C), 10μm (G-P).

Figure 4. *Ctip1* represses motor identity in sensory cortex subcerebral and corticothalamic projection neurons.

(A-F) *Ctip1* is necessary for corticothalamic axons from somatosensory cortex to repress motor identity and project specifically to sensory thalamic nuclei. Schematic of AAV labeling approach (A). In wild-type mice, axons anterogradely labeled by AAV injection into motor or somatosensory cortex sort into VL (motor; red) or VP (sensory, green) (B, C), but axons from *Ctip1*$^{fl/fl}$*;Emx1-Cre* somatosensory cortex project to both VL and VP (D, E). Extent of AAV-

tdTomato and AAV-EGFP labeling is indicated by red and green arrowheads, respectively. Quantification of normalized fluorescence intensity, demonstrating significantly more overlap between motor and somatosensory injections in *Ctip1*$^{fl/fl}$*;Emx1-Cre* mutants (F). **, p<0.01

(G-L) *Ctip1* is not required for corticothalamic axons from distinct sensory areas to sort into appropriate sensory thalamic nuclei. Schematic of AAV labeling approach (G). In wild-type mice, axons anterogradely labeled by AAV injection into somatosensory and visual cortex project to distinct thalamic nuclei in both wild-type (H-I) and *Ctip1*$^{fl/fl}$*;Emx1-Cre* (J-K) mice. Visual cortex CThPN (red) project to dLG, while somatosensory cortex CThPN (green) project to VP. Extent of AAV-tdTomato and AAV-EGFP labeling is indicated by red and green arrowheads, respectively. Quantification of normalized fluorescence intensity, demonstrating minimal overlap between somatosensory and visual injections in both wild-type mice and *Ctip1*$^{fl/fl}$*;Emx1-Cre* mutants (L).

(M-W) *Ctip1* is required for repression of motor identity by visual subcerebral projection neurons. Schematic of labeling approach (M). P1 injection of AAV-tdTomato into motor cortex and AAV-EGFP into visual cortex labels descending projections in P21 wild-type (N-O) and *Ctip1*$^{fl/fl}$*;Emx1-Cre* (S-T) cortex. Motor cortex SCPN from both wild-type and *Ctip1*$^{fl/fl}$*;Emx1-Cre* brains project to the cerebral peduncle in the midbrain (P, U), and continue into the pons and spinal cord (Q, V). In wild-type brain, visual cortex SCPN do not project beyond the midbrain (arrow in P', Q'). However, in *Ctip1*$^{fl/fl}$*;Emx1-Cre* brains, visual cortex SCPN aberrantly project past the midbrain to enter the pons (arrow in U'), then continue into the spinal cord (V'). Axons from motor cortex SCPN project to deep layers of the superior colliculus in wild-type and *Ctip1*$^{fl/fl}$*;Emx1-Cre* brains (R and W). Axons from visual cortex SCPN project exclusively to superficial layers of the superior colliculus in wild-type brains (R'). However, while visual cortex SCPN still project to superficial layers of the superior colliculus in *Ctip1*$^{fl/fl}$*;Emx1-Cre* brains, they also aberrantly innervate deep layers (arrows in W').

dLG, dorsal lateral geniculate nucleus of thalamus; M1, primary motor cortex; S1, primary

somatosensory cortex; SC, superior colliculus; Sp, spinal cord; V1, primary visual cortex; VL, ventral lateral nucleus of thalamus; VP, ventral posterior nucleus of thalamus

Scale bars: 500μm (B, H), 200μm (D-F, I-K)

Figure 5. Postnatal overexpression of *Ctip1* causes motor area SCPN to prune their spinal axons by P21.

(A-C) Schematic of experimental approach (A). Control wild-type embryos were electroporated at E12.5 with CAG-ER^{T2}CreER^{T2}, CAG-FLEX-FlpO, and CAG-FRT-STOP-FRT-EGFP, while experimental embryos were electroporated with these same plasmids, as well as CAG-FRT-STOP-FRT-*Ctip1*. Electroporated pups were injected with tamoxifen at P2, enabling ER^{T2}-CreER^{T2} to invert the orientation of FlpO, activating FlpO expression (B). FlpO then activates expression of both CTIP1 and EGFP in turn (C). Mice were perfused at P21.

(D-L) In control animals, motor cortex electroporations (D-E) result in many axons projecting through the cerebral peduncle (F), and continuing into cervical spinal cord (G). In experimental animals, motor cortex electroporations (H and I) similarly result in many axons projecting through the cerebral peduncle (J). However, very few axons continue into the cervical spinal cord (K), indicating that most *Ctip1*-overexpressing motor cortex SCPN have pruned their spinal collaterals. Quantification (L). n.s., not significant; **, $p<0.01$

Scale bars: 500μm (D, H), 200μm (E-G, I-K).

Figure 6. Cortical *Ctip1* function is required for organization of thalamocortical input into sensory maps.

(A-C) In wild-type P7 cortex, thalamocortical afferents cluster into highly organized maps in somatosensory, visual, and auditory cortex (A), as revealed by serotonin (5HT) immunostaining in flattened cortices. In the absence of cortical *Ctip1* function, however, almost no discernible organization exists (B). Despite the extreme disorganization of thalamocortical input to

Ctip1$^{fl/fl}$*;Emx1-Cre* cortex, the relative size of the motor and sensory domains does not change (C).

(D-I) Sensory maps in thalamic and brainstem nuclei that convey information from whiskers develop in the absence of cortical *Ctip1* function, but later attenuate. Cytochrome oxidase-stained barrelettes in brainstem (schematic, D) are well-organized in both wild-type and *Ctip1*$^{fl/fl}$*;Emx1-Cre* mice (E, F). Barreloids in the ventral posterior nucleus of thalamus (schematic, G) are smaller in *Ctip1*$^{fl/fl}$*;Emx1-Cre* (I) compared with wild-type (H), potentially as a result of "top-down" plasticity, though clear organization is still evident.

(J-S) Thalamic barreloids atrophy in the absence of cortical *Ctip1* function following initial appropriate development. At P0, VB and dLG are the same size in wild-type and *Ctip1*$^{fl/fl}$*;Emx1-Cre* thalamus (outlines, J-K), but by P7, *Ctip1*$^{fl/fl}$*;Emx1-Cre* VB and dLG have atrophied in comparison with wild-type VB and dLG (outlines, L-M). Quantification (N). This atrophy is due in part to apoptosis, which occurs at higher rates in *Ctip1*$^{fl/fl}$*;Emx1-Cre* sensory thalamus than in wild-type (O-S). **, $p<0.01$.

A1, auditory cortex; CC3, cleaved caspase 3; dLG, dorsal lateral geniculate nucleus of thalamus; fl, forelimb; hl, hindlimb; ll, lower lip; lw, large whiskers; M, motor cortex; S, sensory cortex; SpV, spinal trigeminal nucleus; sw, small whiskers; V1, primary visual cortex; VP, ventral posterior nucleus of thalamus

Scale bars: 500μm (A and B), 200μm (E-I), 100μm (J-P).

Figure 7. Layer IV granule neuron differentiation is impaired in the absence of *Ctip1* function, and cell-autonomous loss of *Ctip1* function leads to their exclusion from barrels.

(A-D) At P7, wild-type layer IV granular neurons are oriented into barrel structures visible by DAPI staining (A) or *Rorb* expression (C) in tangential sections. In layer IV of *Ctip1*$^{fl/fl}$*;Emx1-Cre* cortex, neurons do not organize into barrels (B) or express *Rorb* in periodic clusters (D).

(E-L) Genes expressed in barrel cortex by wild-type layer IV granule neurons, including *Rorb*

(E), *Mdga1* (F), *Grm4* (G), and *Dbp* (H), are expressed in *Ctip1*$^{fl/fl}$*;Emx1-Cre* barrel cortex at reduced levels (I) or absent entirely (J-L).

(M-R) In the absence of *Ctip1* function, axons of contralateral CPN compete with thalamocortical axons for synaptic partners in layer IV. Schematic of approach (M). CPN terminals are labeled with AAV-EGFP injected into the contralateral hemisphere, and thalamocortical axon terminals ($ThCN_{VB}$) are labeled with 5HT immunostaining. Wild-type layer IV granule neurons are receptive to synaptic contact with thalamocortical axons (N) and avoid contact with contralaterally-projecting CPN (P). In contrast, *Ctip1*$^{fl/fl}$*;Emx1-Cre* layer IV neurons attract few $ThCN_{VB}$ axon terminals (O), and layer IV is instead occupied by CPN axon terminals (Q). Quantification of 5HT and EGFP fluorescence as percentage of maximum fluorescence intensity (R).

(S-W) Mosaic loss of *Ctip1* function causes layer IV neurons and their dendrites to be excluded from barrels. Wild-type layer IV neurons electroporated with Cre primarily populate barrels (T-T'', W-W''), but *Ctip1*$^{fl/fl}$ neurons electroporated with Cre are excluded from barrels (U-U'', X-X''). Schematic of experimental approach (S) and quantification (V, measuring across dashed boxes in W', X').

Scale bars: 200μm (A-D and T-U), 100μm (E-Q).

Figure 8. *Ctip1* functions independently of *Couptf1*, and restoring expression of *Ctip1* in layer IV of *Ctip1*$^{fl/fl}$*;Emx1-Cre* cortex is sufficient to rescue sensory map formation.

(A-I) CTIP1 and COUPTF1 act sequentially to regulate the position and topography of sensory maps. In wild-type somatosensory cortex, thalamocortical afferents and clusters of *Rorb*-expressing neurons form barrels (A, D-E). In *Couptf1*$^{fl/fl}$*;Emx1-Cre* cortex, sensory representations are miniaturized, and shifted to the caudal extreme of cortex, but maintain their periodic organization (B, F-G). In double mutant *Ctip1*$^{fl/fl}$*;Couptf1*$^{fl/fl}$*;Emx1-Cre* cortex, sensory representations are shifted caudally, as in *Couptf1*$^{fl/fl}$*;Emx1-Cre* cortex, but are also completely

disorganized, as in *Ctip1*$^{fl/fl}$*;Emx1-Cre* cortex (C, H-I).

(J-P) Schematic of approach (J). CAG-floxed(STOP)-*Egfp* and CAG-floxed(STOP)-*Ctip1* are co-electroporated into E14.5 *Ctip1*$^{fl/fl}$*;Emx1-Cre* cortex, and electroporated brains are recovered and flatmounted at P7. *Ctip1*$^{fl/fl}$*;Emx1-Cre* barrel cortex electroporated with EGFP alone contains neither clustering of electroporated neurons nor discernible periodic organization of thalamocortical afferents (K-M, insets in L and M), but *Ctip1*$^{fl/fl}$*;Emx1-Cre* barrel cortex electroporated with both EGFP and *Ctip1* contains clustered electroporated neurons and rudimentary barrel-like structures in barrel cortex (N-P, insets in O and P), indicating that mosaic *Ctip1* misexpression partly compensates for cortex-wide loss of *Ctip1* function.

(Q) Model. *Ctip1* is expressed in sensory cortical areas, and controls sensory area gene expression, output connectivity, and establishment of receptive fields for sensory input connectivity.

Scale bars: 500μm (A-C) and 200μm (D-I).

CTIP1

CTIP1

A

A'

A''

E15.5

medial

lateral

A'

A''

CP

IZ

CP

IZ

B

B'

B''

E15.5

caudal

rostral

B'

B''

CP

IZ

CP

IZ

schematic

CTIP1

C

M1

S1

D

D'

D''

P7

D'

D''

II/III

IV

V

VI

SP

II/III

V

VI

SP

schematic

CTIP1

E

V1

S1

M1

A1

F

V1

S1

M1

A1

P7

schematic

wild-type

Ctip1$^{fl/fl}$;*Emx1-Cre*

wild-type

Ctip1$^{fl/fl}$;*Emx1-Cre*

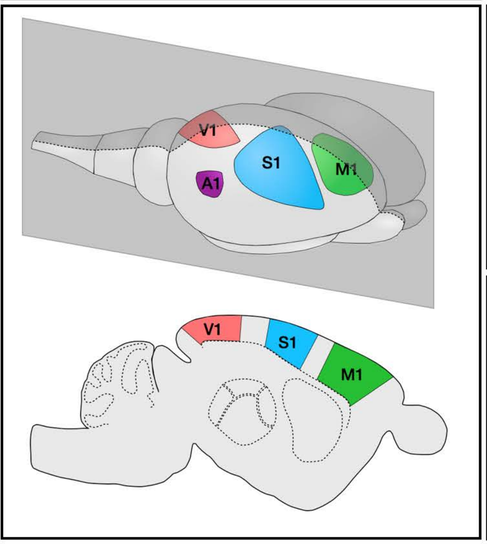

EphA7

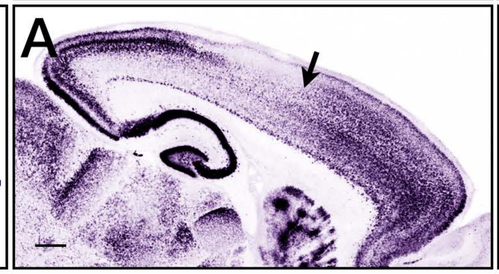

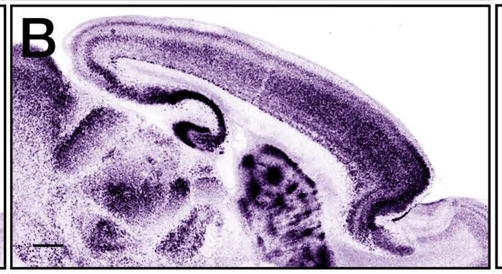

EphrinA5

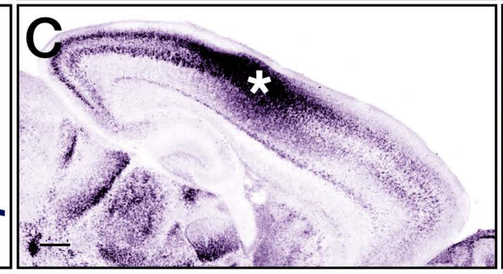

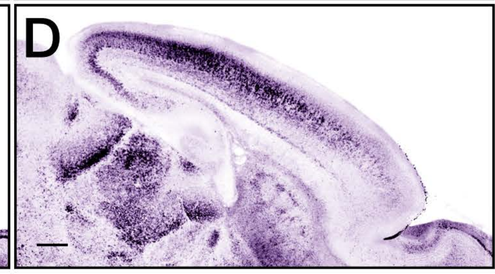

Cdh6

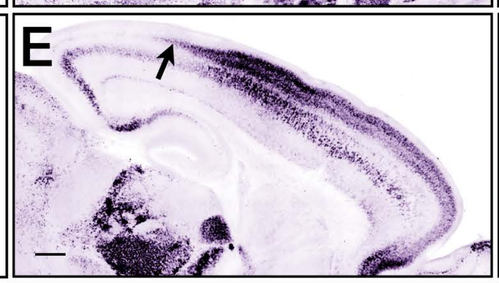

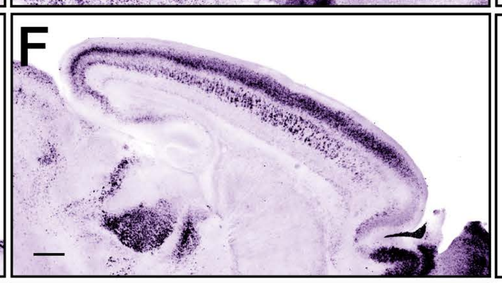

Id2

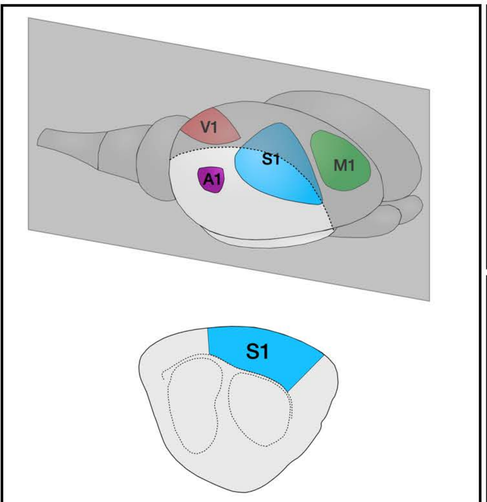

Cyp26b1

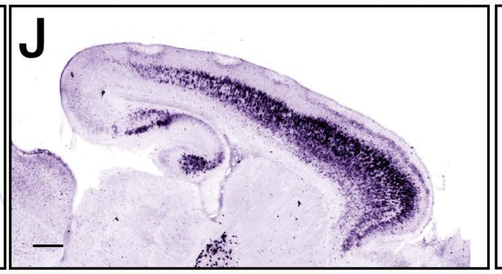

Mdga1

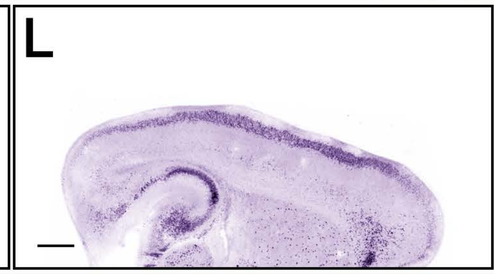

Bhlhe40

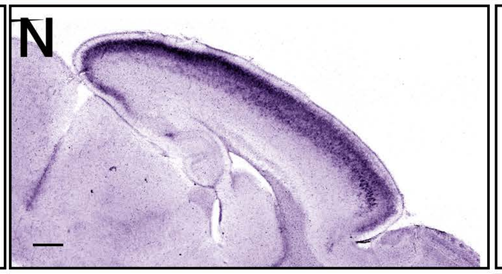

Cux1

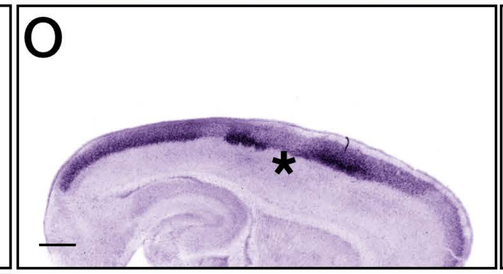

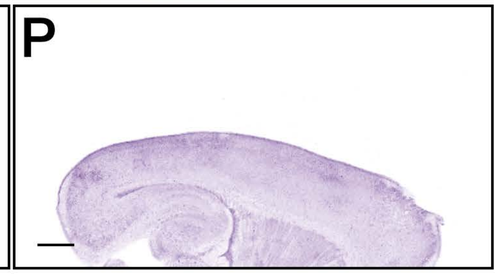

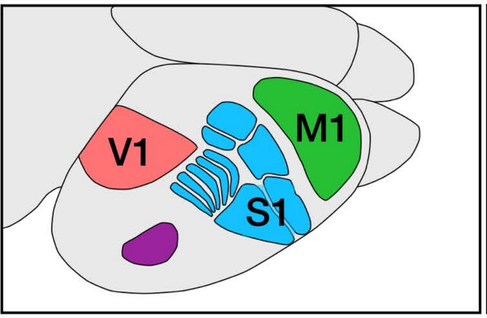

Lmo4-LacZ

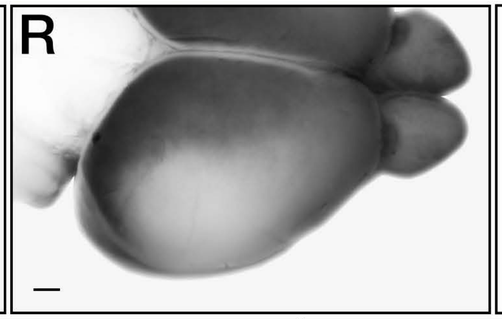

Bhlhb5-LacZ

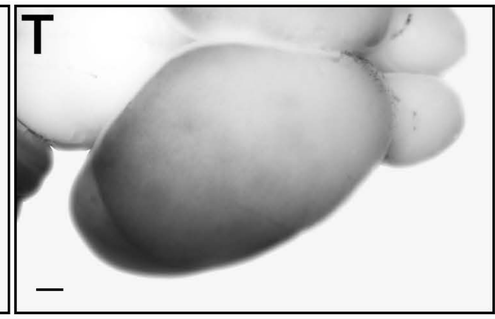

U Identification of area-specific genes in wild-type cortex

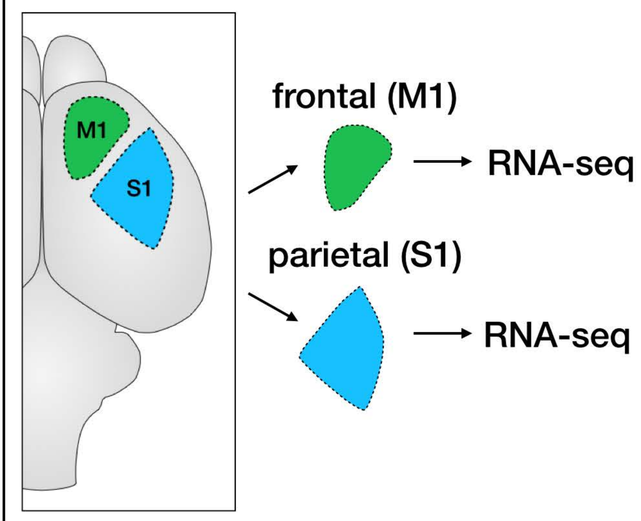

V Gene expression analysis in *Ctip1* cKO parietal cortex

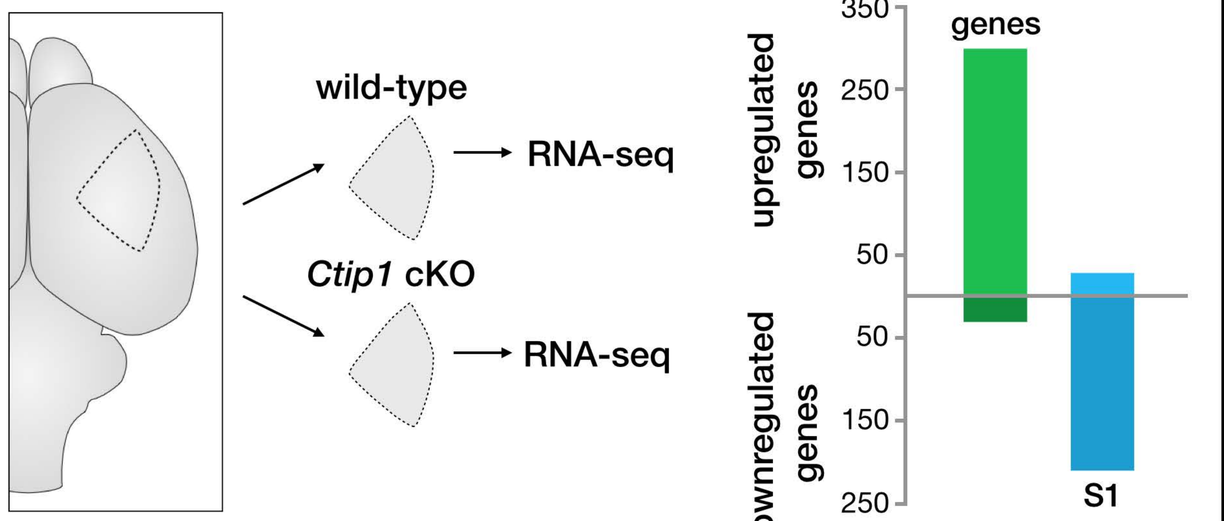

schematic

wild-type

Ctip1$^{fl/fl}$

A

CAG Cre

CAG STOP EGFP

Ep. side

CL side

0

M1/M2

S1FL

S1J

S1UL

S2

Ins.

200

B

0

200

P7

C

0

200

P7

D

electroporated side

M1/M2 S1FL S1J S1ULp S2 Ins. Cx.

norm. fluorescence intensity (%)

WT

Ctip1$^{fl/fl}$

medio-lateral position (bins)

E

contralateral side

M1/M2 S1FL S1J S1ULp S2 Ins. Cx.

norm. fluorescence intensity (%)

WT

Ctip1$^{fl/fl}$

medio-lateral position (bins)

F

WT

Ctip1$^{fl/fl}$

norm. fluorescence intensity (%)

*

n.s.

M1/M2 S1FL S1J S1ULp S2 Ins. Cx.

cortical areas

M1/M2

S1FL

S1J

S1ULp

Ins. Cx.

wild-type

Ctip1$^{fl/fl}$

G H I J K L M N O P

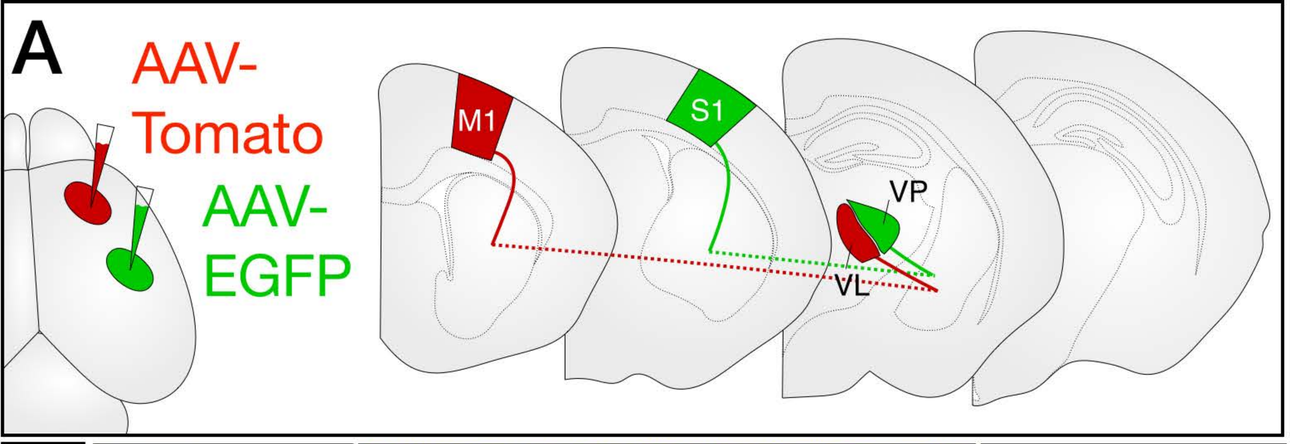
A
AAV-Tomato
AAV-EGFP
M1
S1
VP
VL

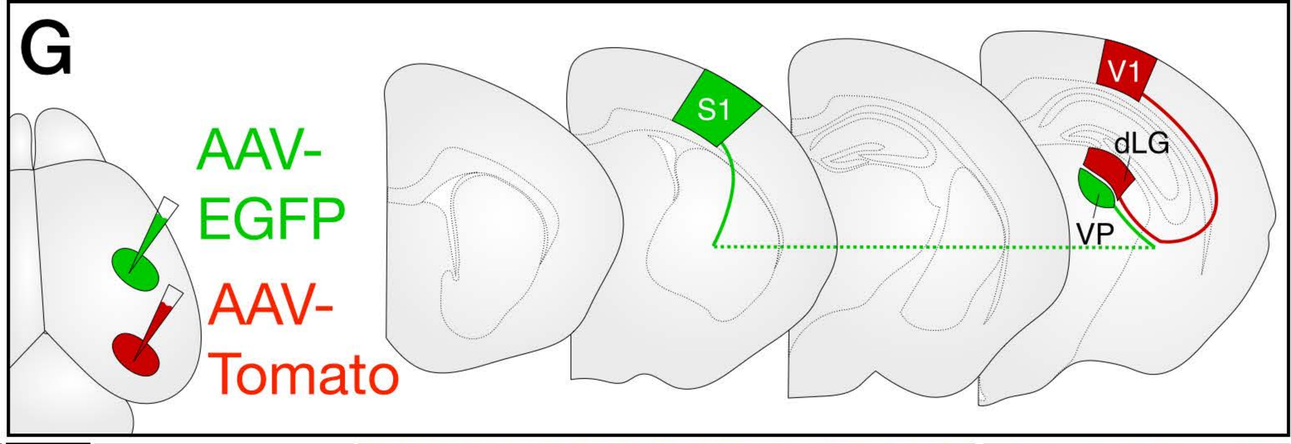
G
AAV-EGFP
AAV-Tomato
S1
V1
dLG
VP

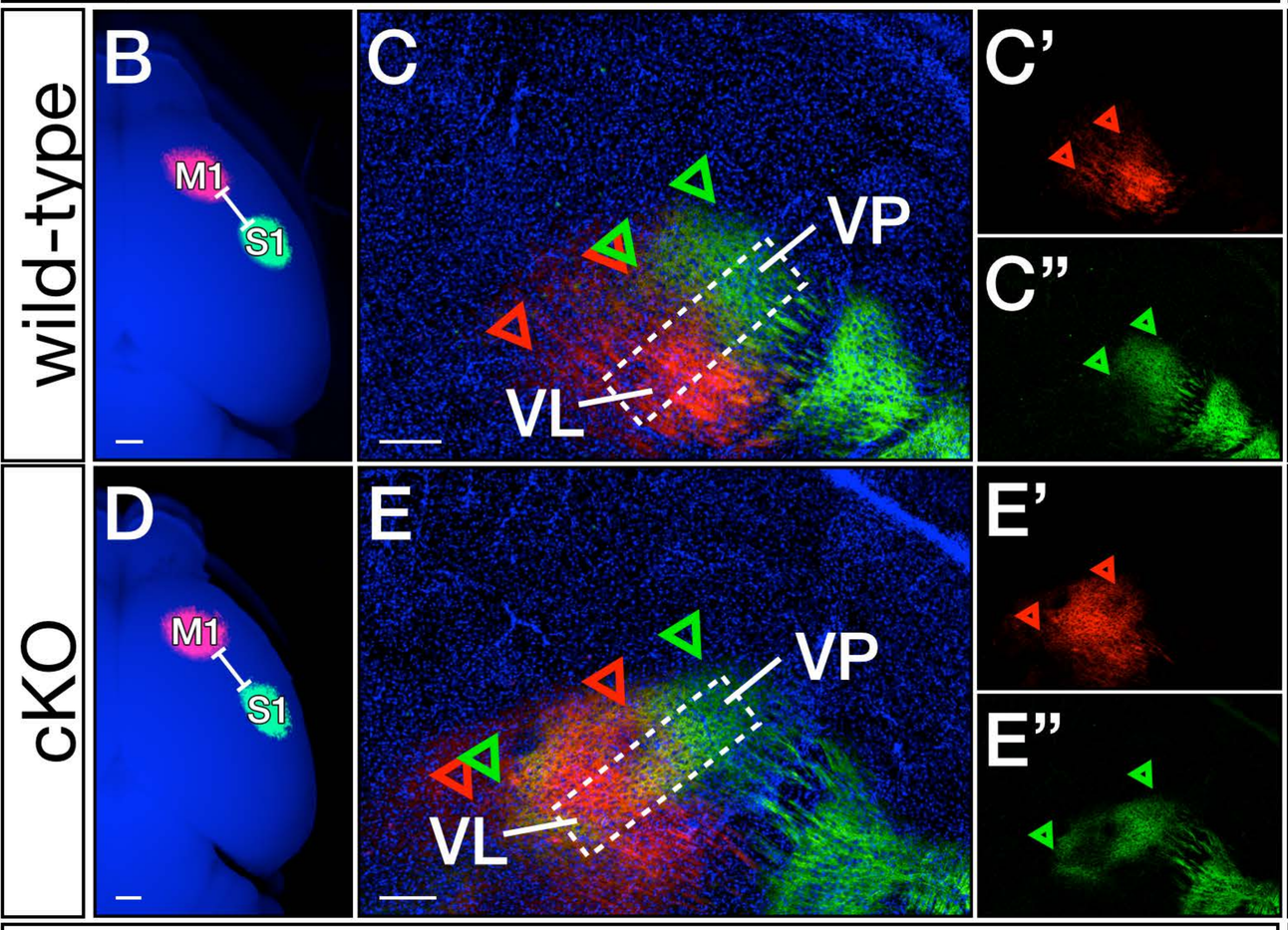
wild-type
cKO
B
C
C'
C''
D
E
E'
E''
M1
S1
VP
VL

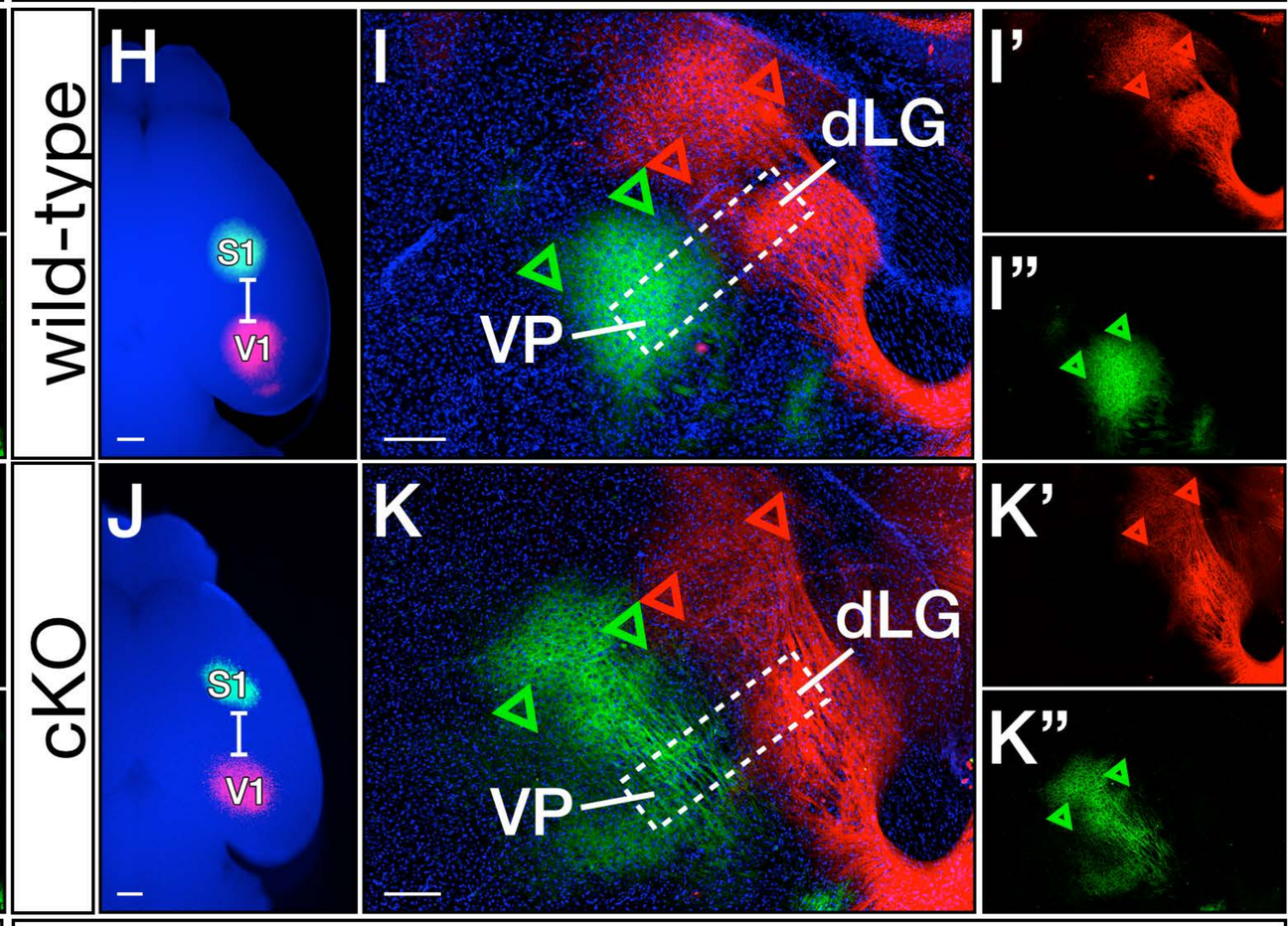
wild-type
cKO
H
I
I'
I''
J
K
K'
K''
S1
V1
dLG
VP

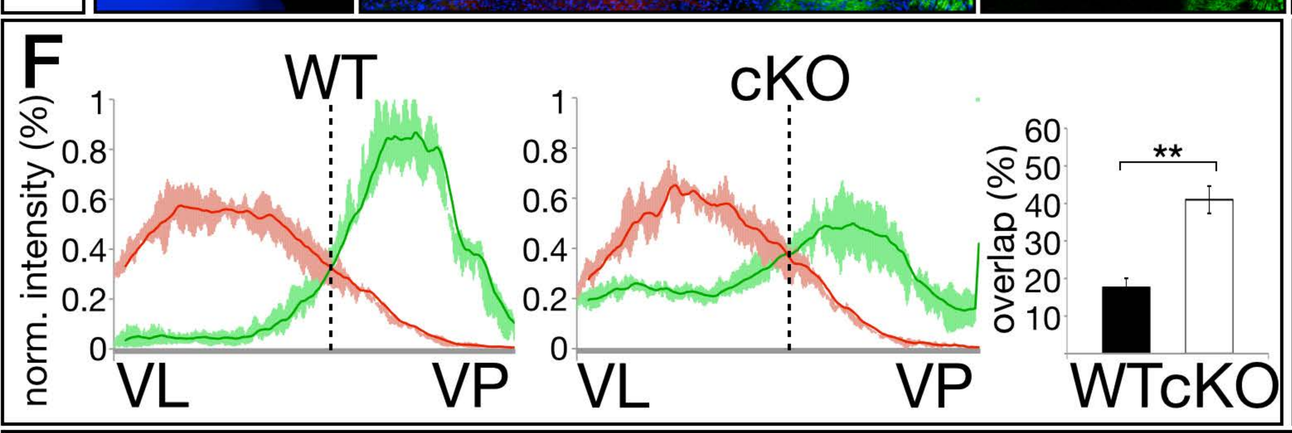
F
WT
cKO
norm. intensity (%)
VL
VP
overlap (%)
**
WTcKO

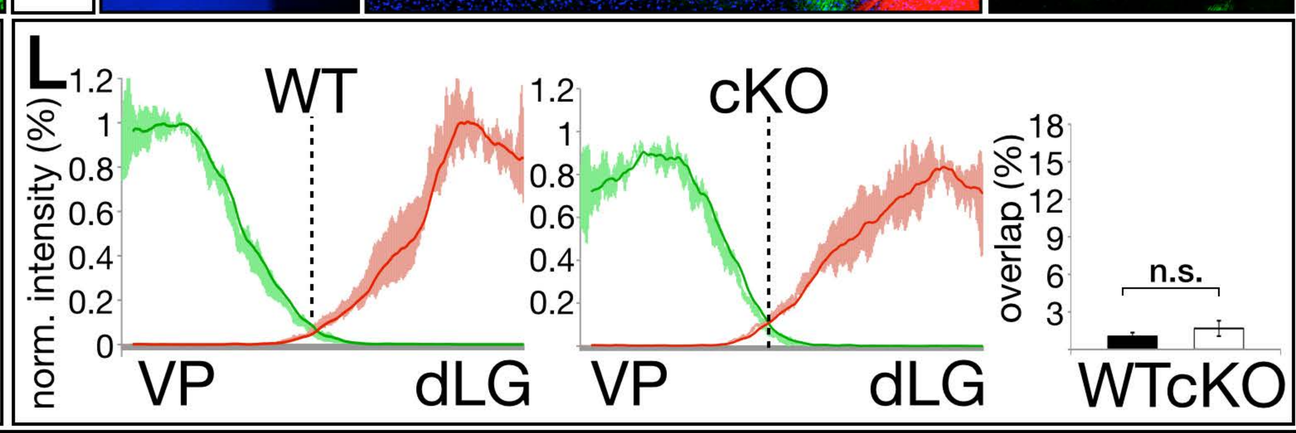
L
WT
cKO
norm. intensity (%)
VP
dLG
overlap (%)
n.s.
WTcKO

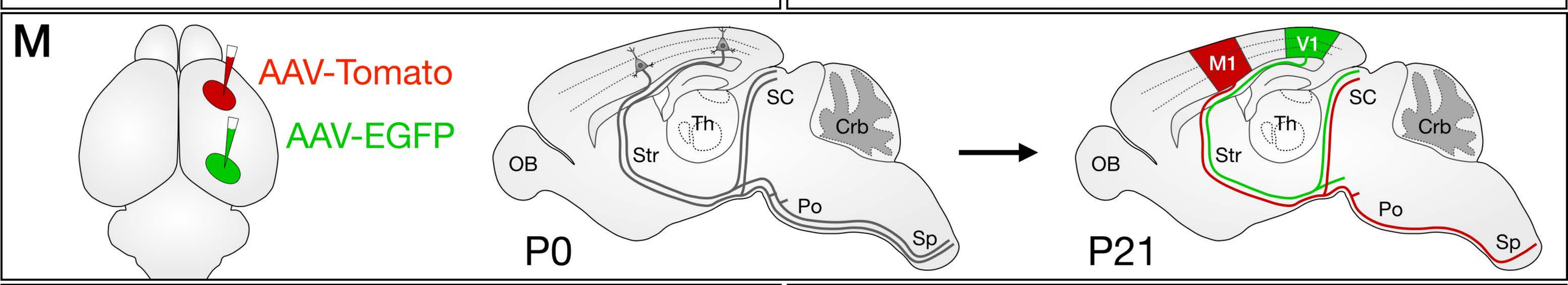
M
AAV-Tomato
AAV-EGFP
OB
Str
Th
SC
Crb
Po
Sp
P0
M1
V1
P21

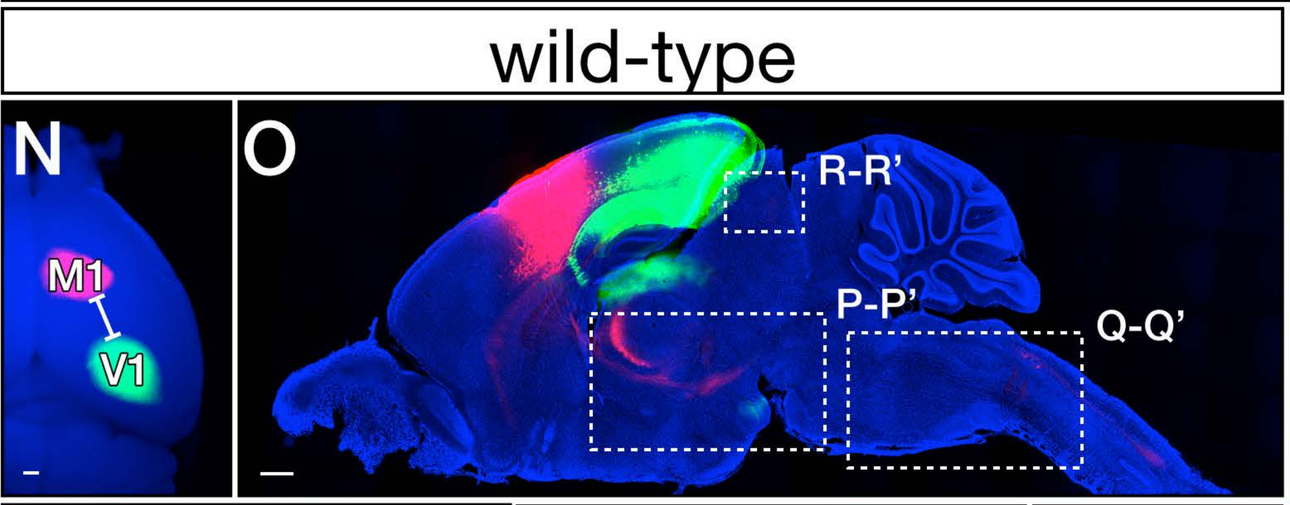
wild-type
N
O
M1
V1
R-R'
P-P'
Q-Q'

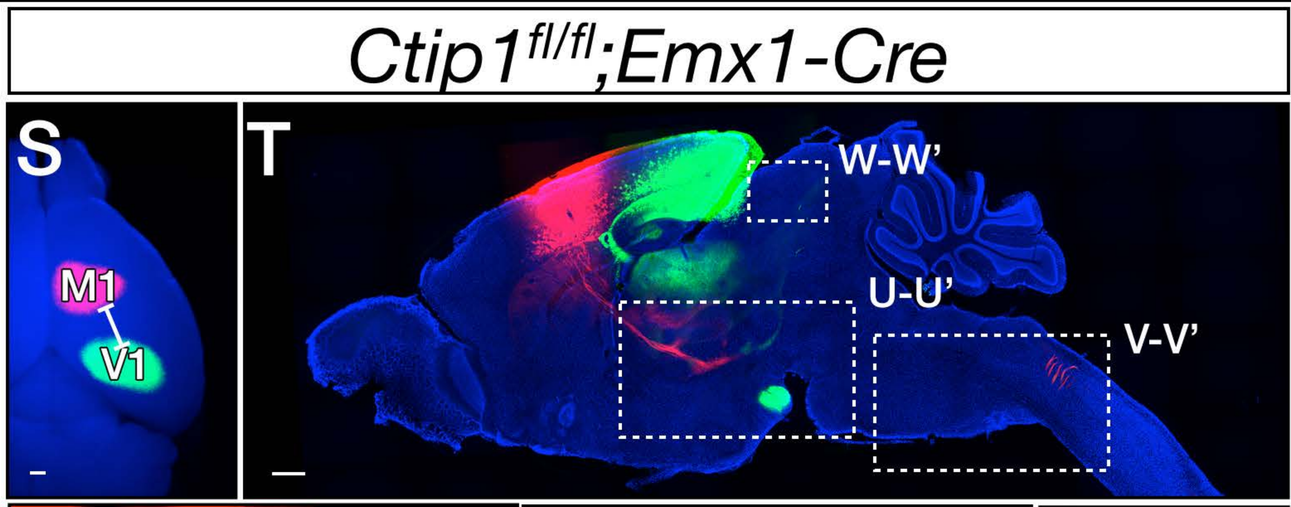
Ctip1fl/fl;Emx1-Cre
S
T
M1
V1
W-W'
U-U'
V-V'

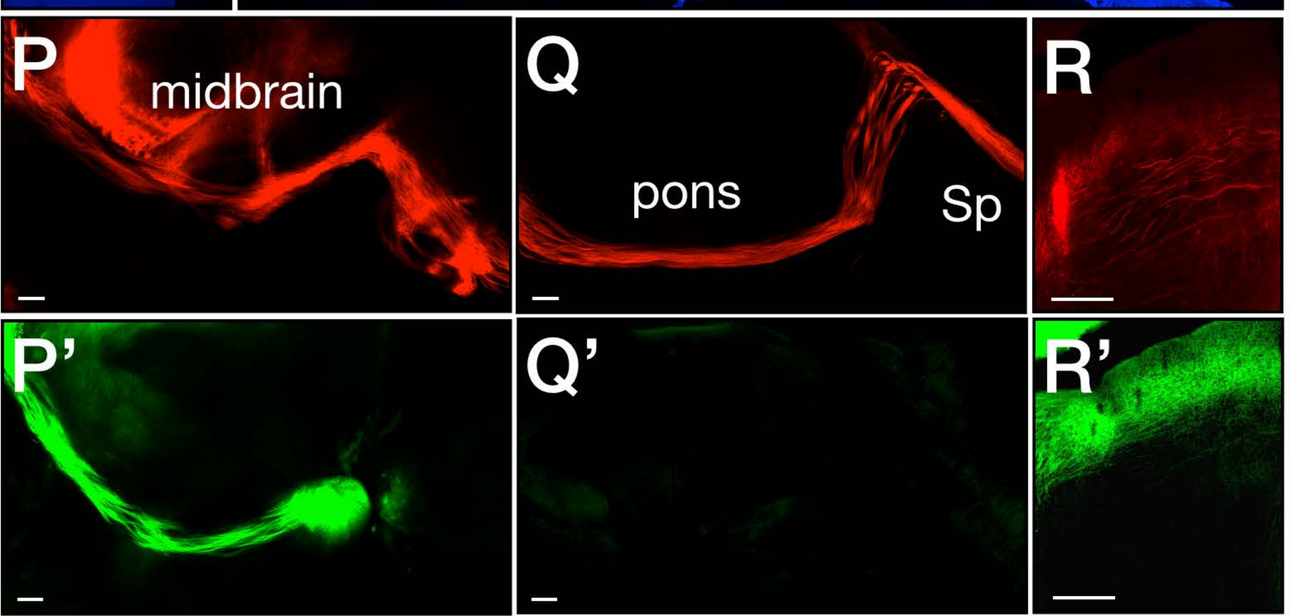
P
midbrain
Q
pons
Sp
R
P'
Q'
R'

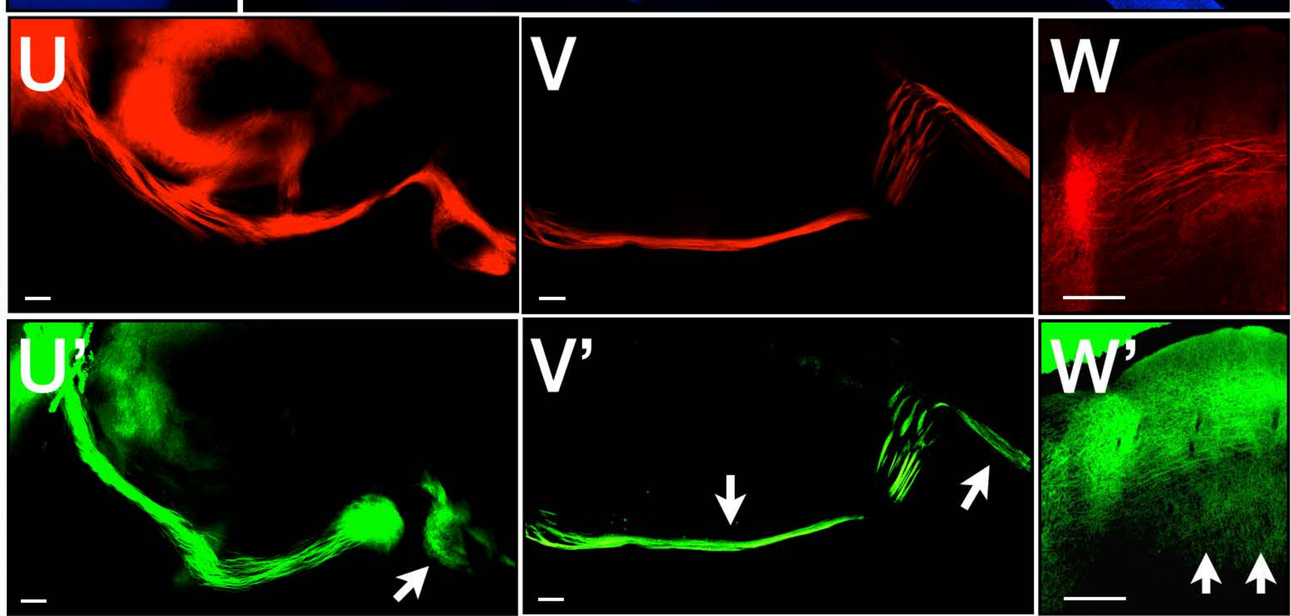
U
V
W
U'
V'
W'

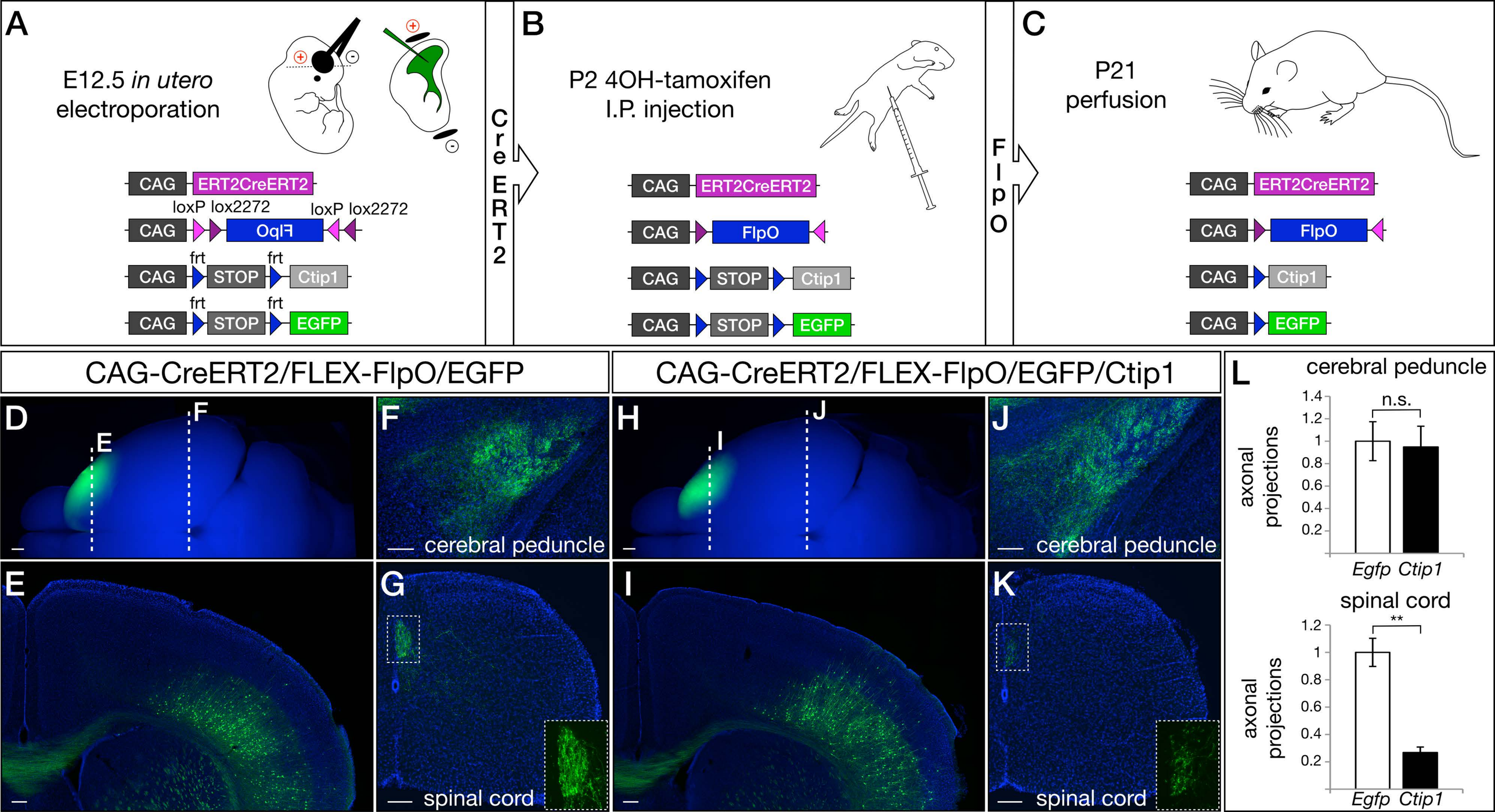
A
E12.5 in utero electroporation
CAG ERT2CreERT2
loxP lox2272 loxP lox2272
CAG FlpO
frt STOP frt
CAG Ctip1
frt STOP frt
CAG EGFP
CreERT2
B
P2 4OH-tamoxifen I.P. injection
CAG ERT2CreERT2
CAG FlpO
CAG STOP Ctip1
CAG STOP EGFP
FlpO
C
P21 perfusion
CAG ERT2CreERT2
CAG FlpO
CAG Ctip1
CAG EGFP
CAG-CreERT2/FLEX-FlpO/EGFP
CAG-CreERT2/FLEX-FlpO/EGFP/Ctip1
D
E
F
F
cerebral peduncle
H
I
J
J
cerebral peduncle
E
G
spinal cord
I
K
spinal cord
L
cerebral peduncle
axonal projections
n.s.
Egfp Ctip1
spinal cord
axonal projections
**
Egfp Ctip1

wild-type | *Ctip1$^{fl/fl}$;Emx1-Cre* | quantification

5HT

A P7 — V1, hl, lw, fl, A1, sw, ll

B P7

C — S, M; M-S ratio = M / S; M-S ratio: 1.0, 0.9, 0.8, 0.7, 0.6, 0.5, 0.4, 0.3, 0.2, 0.1, 0; n.s.; WT, cKO

brainstem (barrelettes) | thalamus (barreloids)

schematic | wild-type | cKO | schematic | wild-type | cKO

D | E P7 spV | F P7 spV | G | H P7 VP | I P7 VP

wild-type | cKO | wild-type | cKO | P7 quantification

J P0 dLG, VP, *Sert* | K P0 VP, *Sert* | L P7 dLG, VP, *Sert* | M P7 VP, *Sert*

N — VB, dLG; relative size: 1.2, 1, 0.8, 0.6, 0.4, 0.2, 0; **; WT, cKO, WT, cKO

wild-type | cKO | wild-type | cKO

O P1 VP, CC3 / DAPI | P P1 VP, CC3 / DAPI | Q | R

S — VB, dLG; CC3+ cells/mm^2: 400, 350, 300, 250, 200, 150, 100, 50, 0; **; WT, cKO, WT, cKO

wild-type | *Ctip1$^{fl/fl}$;Emx1-Cre* | wild-type | *Ctip1$^{fl/fl}$;Emx1-Cre*

A DAPI | B DAPI | C *Rorb* | D *Rorb*

wild-type | *Ctip1$^{fl/fl}$;Emx1-Cre*

E *Rorb* | F *Mdga1* | G *Grm4* | H *Dbp* | I *Rorb* | J *Mdga1* | K *Grm4* | L *Dbp*

II/III, IV, V, VI

M

α5HT — ThCN$_{VB}$ term.

AAV-EGFP — CPN term.

WT | cKO | WT | cKO

N 5HT | O 5HT | P EGFP | Q EGFP

R 5HT | EGFP

radial position (bins) 0–200

fluorescence intensity (%) 20 40 60 80

cKO | WT

S E14.5 P7

flatmount

CAG Cre

CAG STOP EGFP

wild-type

T RORB | T' EGFP | T'' V-V''

Ctip1$^{fl/fl}$

U RORB | U' EGFP | U'' W-W''

V

EGFP fluorescence intensity (%) 0 0.2 0.4 0.6 0.8 1

sp. barrel sp.

WT

Ctip1$^{fl/fl}$

medio-lateral position (bins) 0 200

wild-type

W | W' | W''

Ctip1$^{fl/fl}$

X | X' | X''

wild-type

Couptf1$^{fl/fl}$;*Emx1-Cre*

Couptf1$^{fl/fl}$;*Ctip1*$^{fl/fl}$;*Emx1-Cre*

P7

V1

S1

A1

A

5HT

B

C

D

5HT

E

Rorb

F

G

H

I

J

E14.5

CAG STOP EGFP

CAG STOP Ctip1

Ctip1$^{fl/fl}$;*Emx1-Cre*

P7

control Ep

layer IV rescue electroporation

II/III

IV

V

VI

Ctip1 Ep

control Ep into cKO

Ctip1 Ep into cKO

K

L

M

N

O

P

5HT/EGFP

Q *Ctip1* expression in sensory domain

1. Represses M1 genes and activates S1 genes

Ctip1

OT

Th

SC

2. Directs sensory-specific output connectivity

V1

3. Establishes receptive sensory field in layer IV

Area identity specification

Couptf1

Pax6

Emx2

Sp8

S1

M1

- changes in relative size/position
- normal area differentiation

e.g., *Couptf1* cKO

Area identity acquisition

Ctip1

Lmo4

Bhlhb5

- normal relative size/position
- abnormal differentiation of affected area

e.g., *Ctip1* cKO

Bhlhb5-LacZ

Bhlhb5-LacZ

SUPPLEMENTAL FIGURES

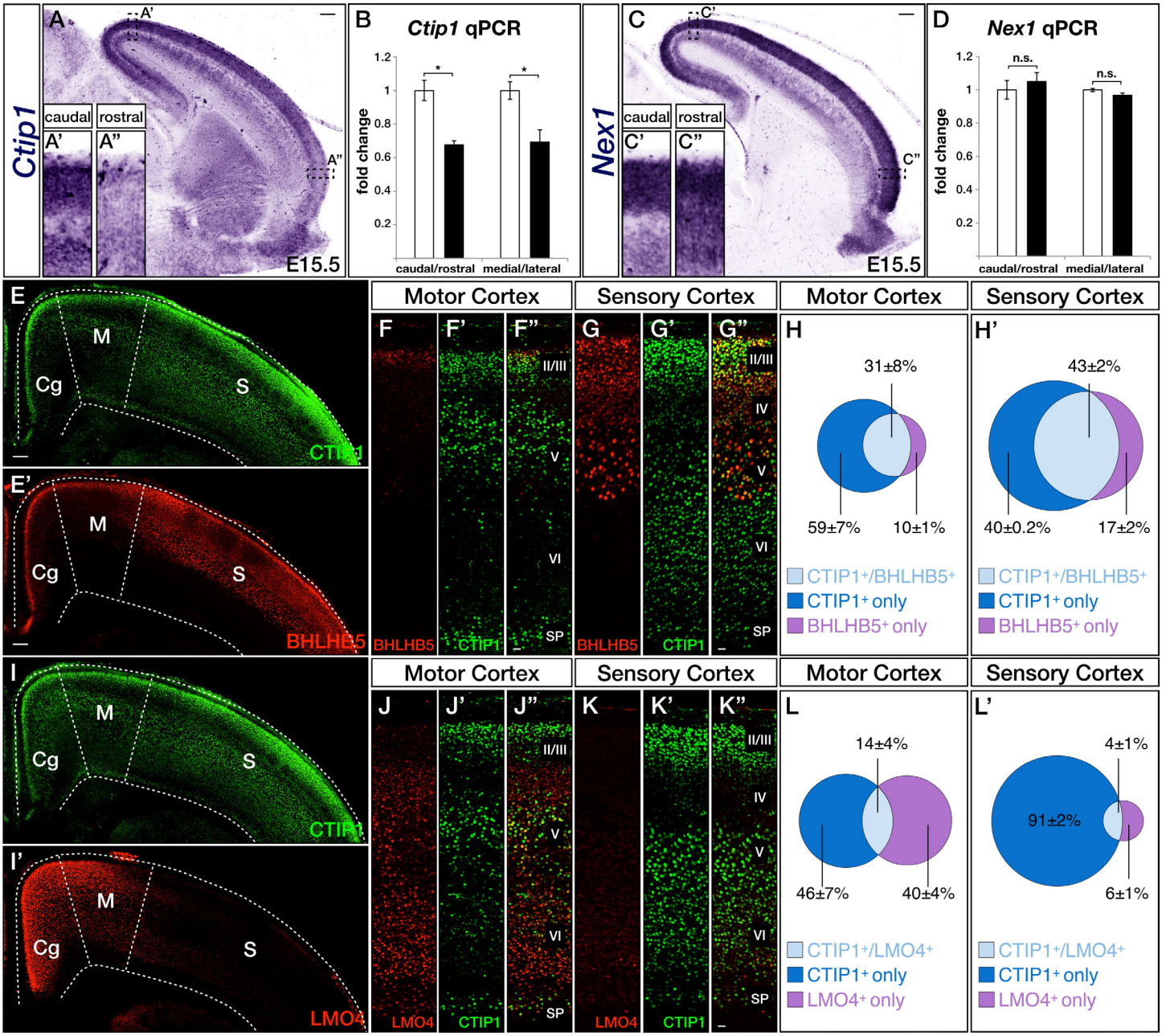

Figure S1. (related to Figure 1) CTIP1 is expressed embryonically in a high-caudomedial to low-rostrolateral gradient, then expressed at P7 at high levels by neurons in somatosensory cortex, and at low levels by neurons in motor cortex.

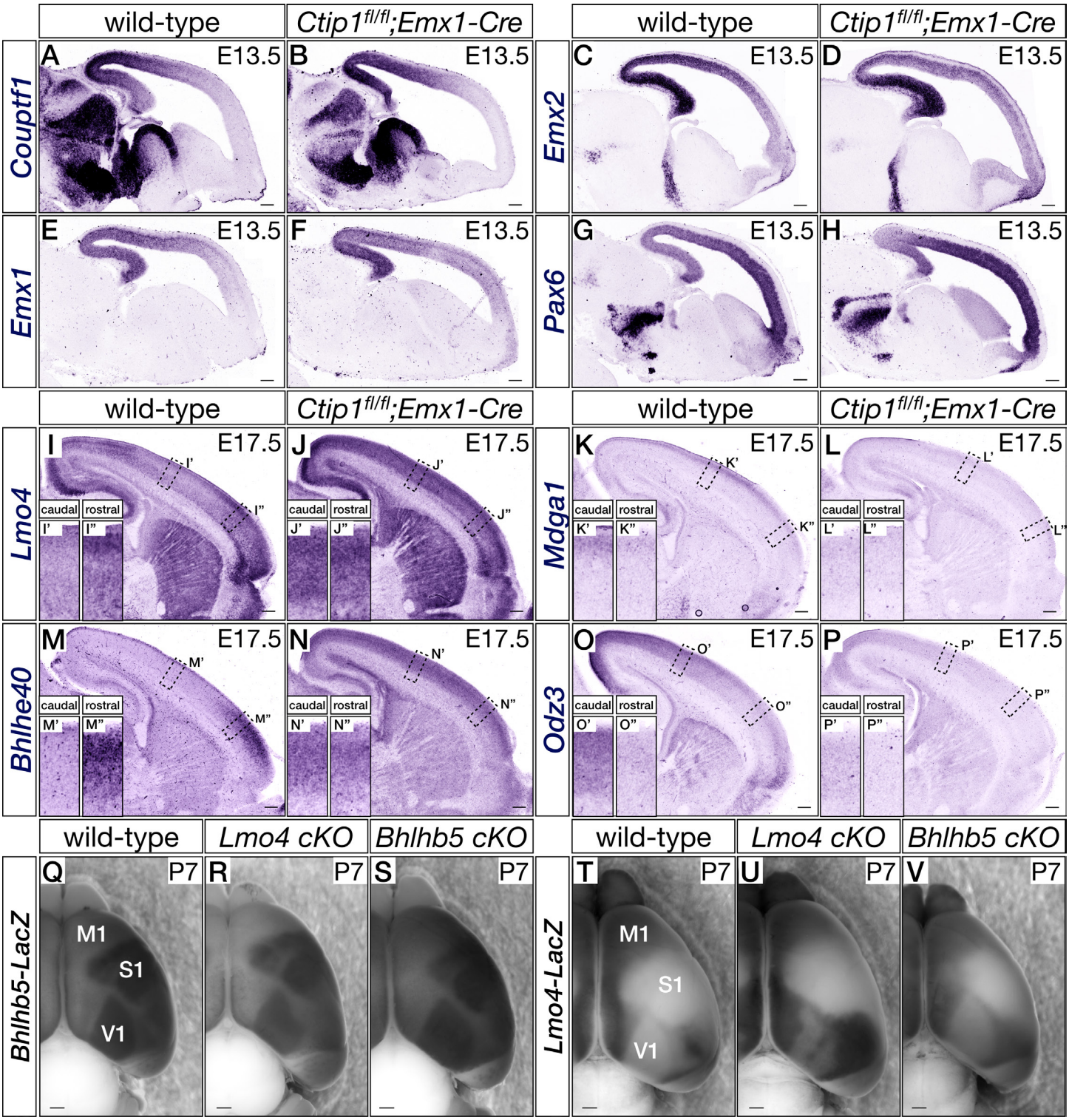

Figure S2. (related to Figure 2) Graded expression of postmitotic areally specified genes, but not progenitor-expressed areally specified genes, is affected by loss of *Ctip1* function.

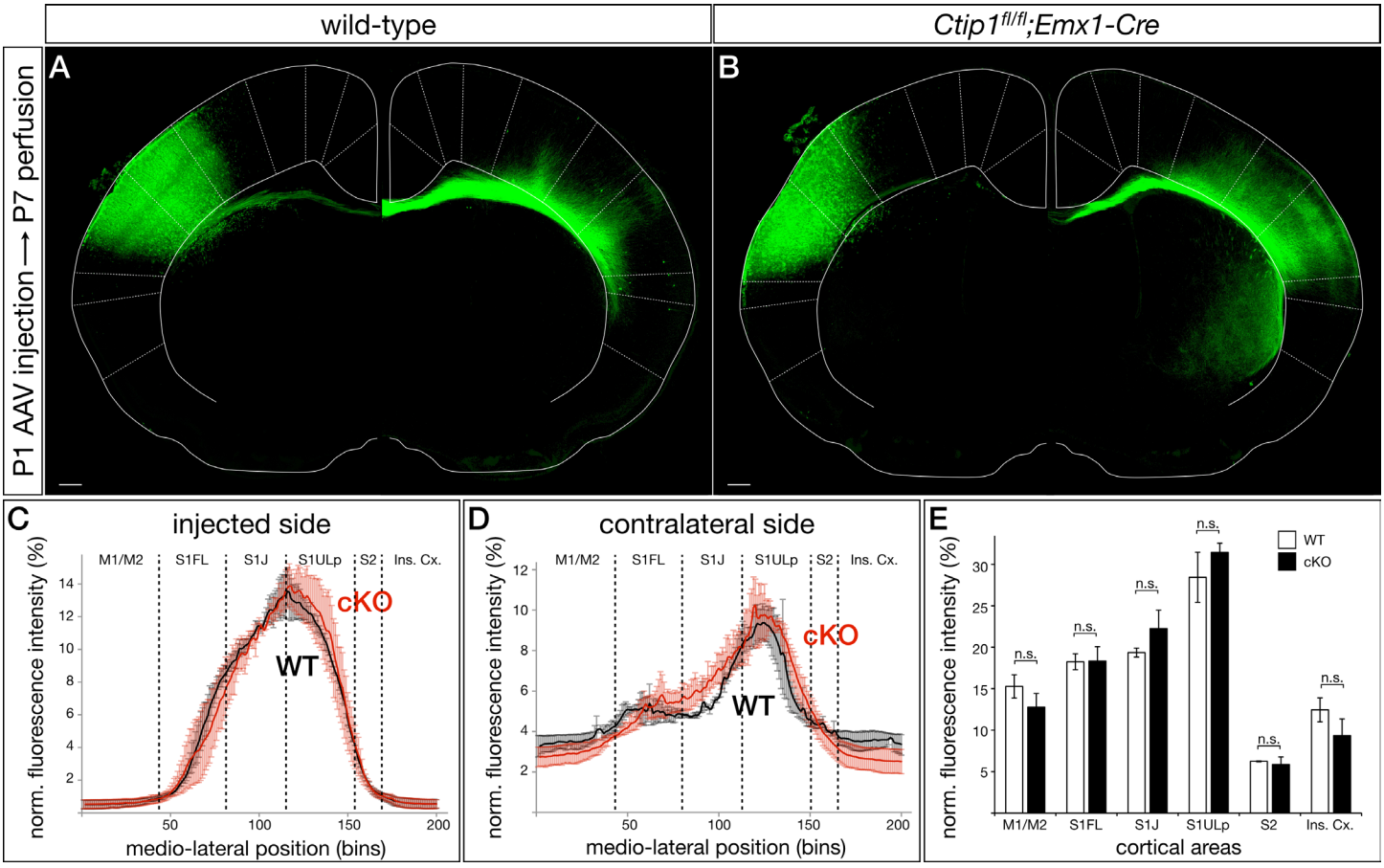

Figure S3. (related to Figure 3) In the absence of cortical *Ctip1* function, CPN aberrantly project to non-homotypic locations on the contralateral hemisphere.

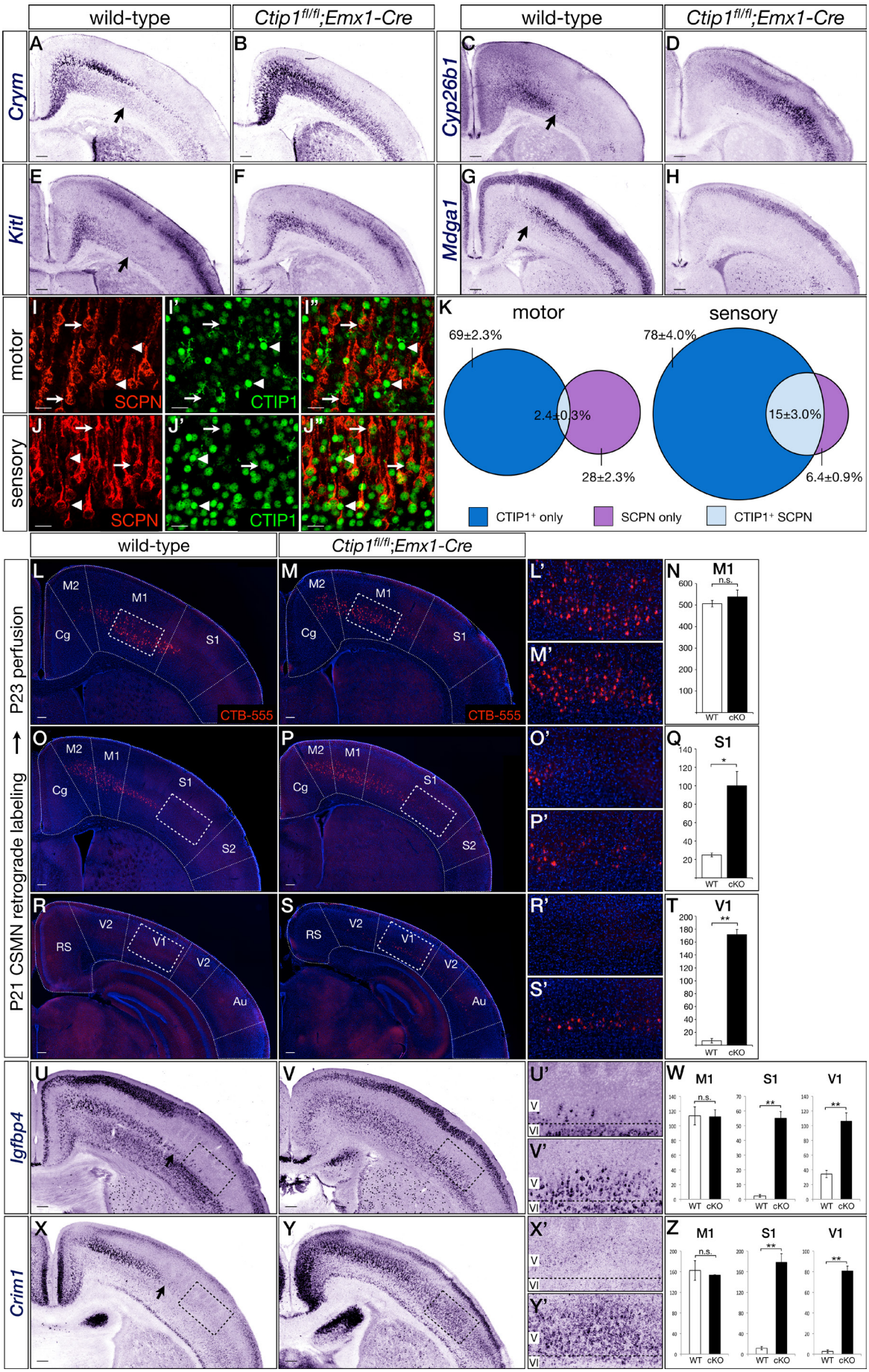

Figure S4. (related to Figure 4) *Ctip1* is required for sensory cortex SCPN and CThPN to repress motor-specific genes, and for sensory cortex SCPN to prune their spinal axons.

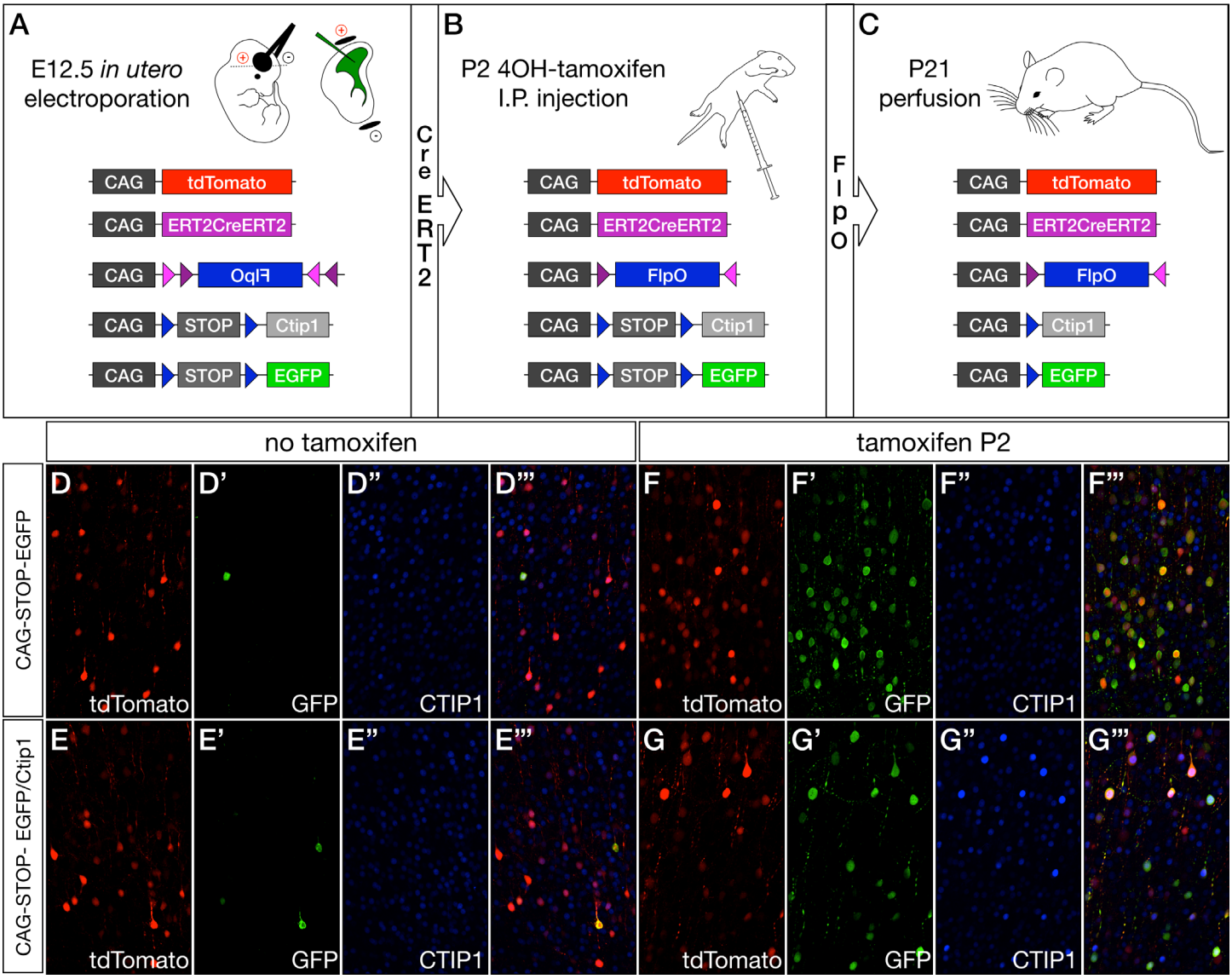

Figure S5. (related to Figure 5) Induction of $ER^{T2}CreER^{T2}$ by tamoxifen injection results in robust postnatal overexpression of CTIP1.

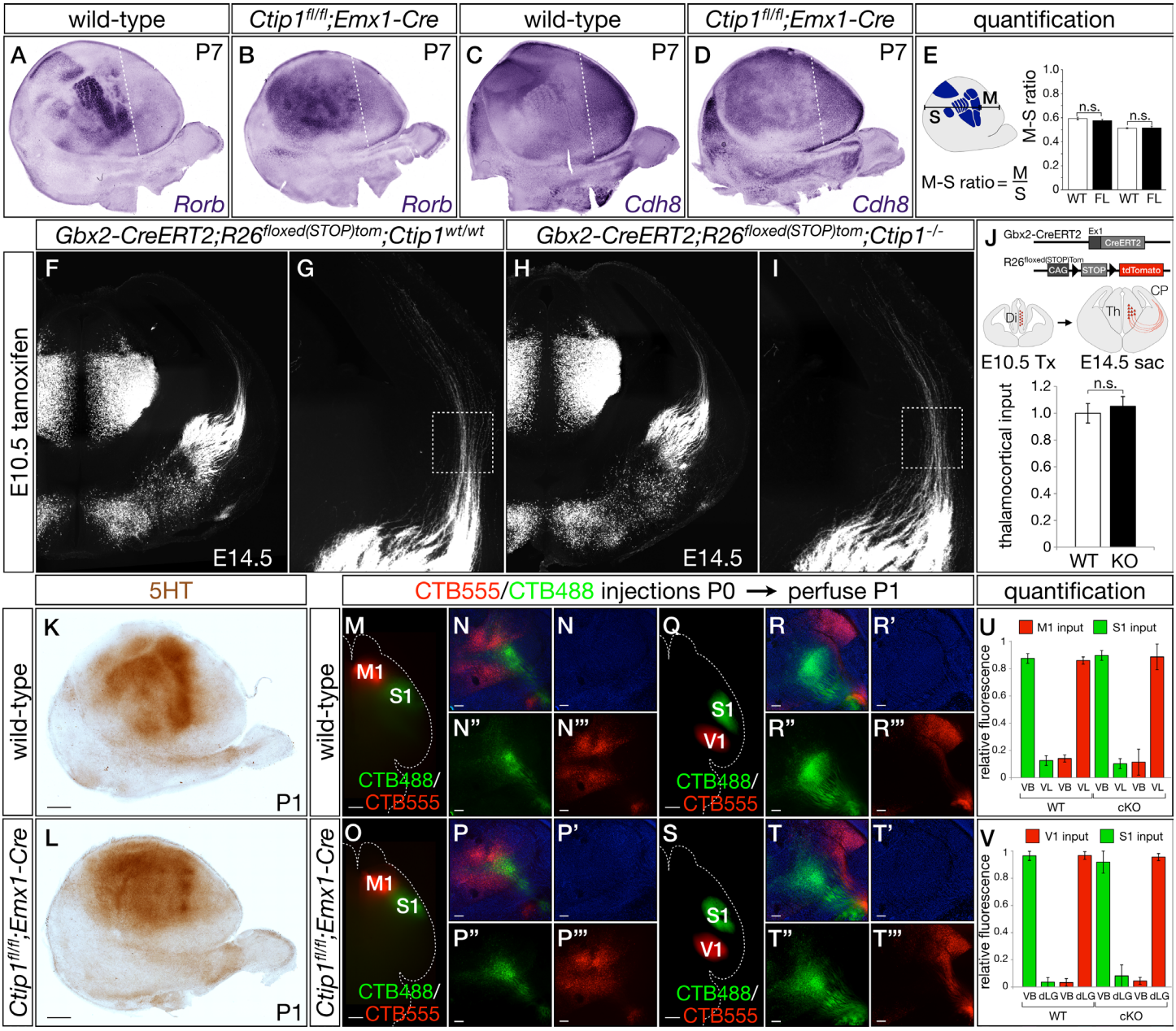

Figure S6. (related to Figure 6) Thalamocortical axons invade appropriate regions of cortex in the absence of *Ctip1*, and induce appropriate cortical gene expression, despite their failure to organize into sensory maps.

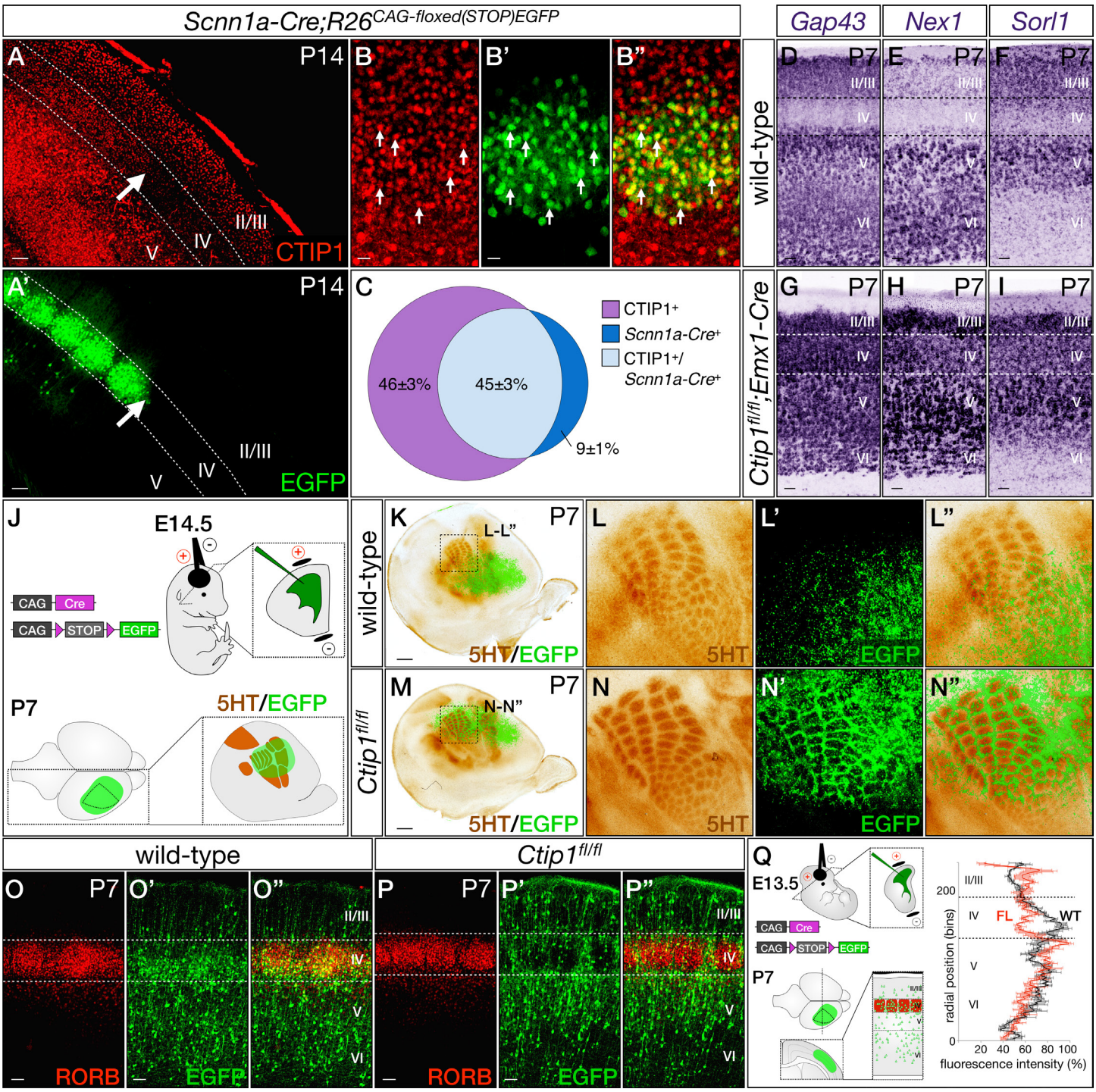

Figure S7. (related to Figure 7) Layer IV granule neurons express CTIP1, and mosaic deletion of *Ctip1* in layer IV does not disrupt sensory map formation.

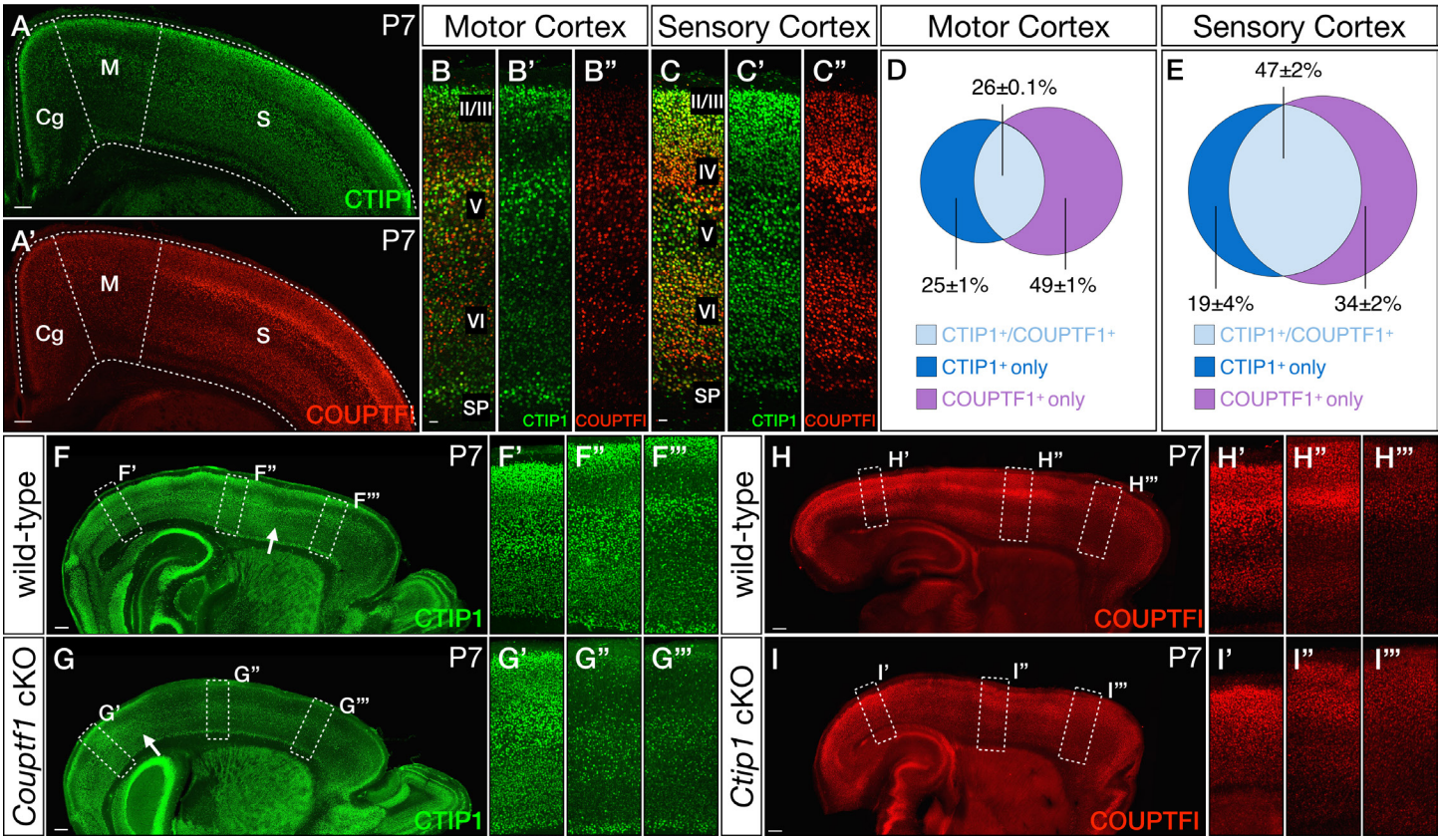

Figure S8. (related to Figure 8) CTIP1 and COUPTFI are extensively co-expressed in sensory cortex, and each regulates expression of the other.

SUPPLEMENTAL FIGURE LEGENDS

Figure S1. (related to Figure 1) CTIP1 is expressed embryonically in a high-caudomedial to low-rostrolateral gradient, then expressed at P7 at high levels by neurons in somatosensory cortex, and at low levels by neurons in motor cortex.
(A-D) *Ctip1* mRNA is expressed at high levels caudally and low levels rostrally, while no such gradient exists for other genes expressed in the embryonic cortical plate, such as *Nex1*. *In situ* hybridization (A, C), quantitative PCR (B, D).
(E-H) CTIP1 and BHLHB5 share similar areal expression patterns in neocortex, and are extensively co-expressed by projection neurons in somatosensory cortex (E-E'). CTIP1 and BHLHB5 are expressed at low levels in cingulate and motor cortex (F-F''), but expression of both transcription factors sharply increases in somatosensory cortex (G-G''). Quantification of expression in motor and sensory cortex (H).
(I-L) Expression of CTIP1 and LMO4 is largely complementary, although some co-expression occurs by individual projection neurons in deep layers of motor cortex (I-I'). LMO4 expression is strongest in cingulate and motor cortex, while CTIP1 is expressed most highly in somatosensory cortex (J-K''). Quantification of expression in motor and sensory cortex (L).
n.s., not significant, *, $p<0.01$.
Scale bars: 100µm (E, I), 25µm (F, G, J, K).

Figure S2. (related to Figure 2) Graded expression of postmitotic areally specified genes, but not progenitor-expressed areally specified genes, is affected by loss of *Ctip1* function.
(A-H) Progenitor-level controls over area identity are expressed in normal rostro-caudal gradients in the absence of *Ctip1* function at E13.5. *Couptf1* (A-B), *Emx2* (C-D), *Emx1* (E-F), and *Pax6* (G-H), important regulators of early area development in the ventricular zone, are present in expected expression gradients in both wild-type and *Ctip1$^{fl/fl}$;Emx1-Cre* cortex at E13.5.
(I-P) Postmitotic markers of area identity are not expressed in normal rostro-caudal gradients in the absence of *Ctip1* function at E17.5. In wild-type cortex, *Lmo4* (I) and *Bhlhe40* (M) are expressed at higher levels rostrally than caudally, and *Mdga1* (K) and *Odz3* (O) are expressed at higher levels caudally than rostrally. In *Ctip1$^{fl/fl}$;Emx1-Cre* cortex, these genes are expressed at relatively uniform levels rostrally and caudally (J, N, L, P).
(Q-V) Area identity is acquired largely normally in the absence of postmitotic area identity controls *Bhlhb5* and *Lmo4* at P7. *Bhlhb5-LacZ* delineates S1 and V1 in wild-type (Q), *Lmo4$^{fl/fl}$;Emx1-Cre* conditional null (R), and *Bhlhb5$^{fl/-}$;Emx1-Cre* conditional null (S) cortex. *Lmo4-LacZ* is absent from S1 and V1 in wild-type (T), *Lmo4$^{fl/-}$;Emx1-Cre* conditional null (U), and *Bhlhb5$^{fl/fl}$;Emx1-Cre* conditional null (V) cortex.
Scale bars: 200µm (A-P), 500µm (Q-V).

Figure S3. (related to Figure 3) In the absence of cortical *Ctip1* function, CPN aberrantly project to non-homotypic locations on the contralateral hemisphere.
In wild-type mice, injection of AAV-EGFP into somatosensory cortex (A) anterogradely labels projections in the contralateral hemisphere that are spatially restricted to homotypic regions, and have distinct clusters in S1FL and S1ULp (D). However, injection of AAV-EGFP into *Ctip1$^{fl/fl}$;Emx1-Cre* somatosensory cortex (B) labels projections that cover a wider area of the contralateral hemisphere, and are mediolaterally more uniform (D), indicating that callosal projections have lost homotypic targeting precision.
Scale bars: 100µm, all panels.

Figure S4. (related to Figure 4) *Ctip1* is required for sensory cortex SCPN and CThPN to repress motor-specific genes, and for sensory cortex SCPN to prune their spinal axons.
(A-H) In wild-type mice, *Crym* (A), *Cyp26b1* (C), and *Kitl* (E) are expressed by corticothalamic projection neurons in sensory cortex, but not in motor cortex (boundary at arrow). In *Ctip1$^{fl/fl}$;Emx1-Cre* cortex, expression of these genes spreads to CThPN in sensory cortex (B, D, F). In addition, sensory CThPN in *Ctip1$^{fl/fl}$;Emx1-Cre* cortex cease to express *Mdga1* (G-H).
(I-K) CTIP1 is expressed at low levels by most SCPN in somatosensory cortex (J-J''), but very few in motor cortex (I-I''). Quantification (K).
(L-T) Mature sensory cortex SCPN maintain a CSMN-like connection with the spinal cord at P23 in the absence of neocortical *Ctip1*. The number of neurons retrogradely labeled from the spinal cord at P21 is the same in wild-type (L, L') and *Ctip1$^{fl/fl}$;Emx1-Cre* (M, M') motor cortex (quantification in N). In somatosensory and visual cortex, however, significantly more neurons are retrogradely labeled from the spinal cord in *Ctip1$^{fl/fl}$;Emx1-Cre* mice (P, P',

S, S') than in wild-type mice (O, O', R, R') (quantification in Q, T). Quantification represents the absolute number of retrogradely labeled neurons counted in four sections at each coronal level in an area of defined size, n=3.
(U-Z) Sensory cortex SCPN express CSMN-specific genes at P4, before SCPN pruning begins. In P4 wild-type mice, *Igfbp4* (U) and *Crim1* (V) are restricted to motor cortex SCPN (CSMN; U', V'). In P4 *Ctip1*$^{fl/fl}$*;Emx1-Cre* mice, however, *Igfbp4* (X) and *Crim1* (Y) expression expands beyond motor cortex and into somatosensory areas (X', Y') Quantification (W, Z).
*, $p<0.05$; **, $p<0.01$; Au, auditory cortex; Cg, cingulate cortex; M1, primary motor cortex; M2, secondary motor cortex; n.s., not significant; S1, primary somatosensory cortex; S2, secondary somatosensory cortex; RS, retrosplenial cortex; SCPN, subcerebral projection neurons; V1, primary visual cortex; V2, secondary visual cortex
Scale bars: 50µm (I-J), 150µm (L-Z).

Figure S5. (related to Figure 5) Induction of ER^{T2}CreER^{T2} by tamoxifen injection results in robust postnatal overexpression of CTIP1.
(A-C) Schematic of experimental approach. Wild-type embryos were electroporated at E12.5 with CAG-ER^{T2}CreER^{T2}, CAG-FLEX-FlpO, CAG-frt-STOP-frt-*Ctip1*, and CAG-frt-STOP-frt-EGFP (A). Electroporated pups were injected with tamoxifen at P2, enabling ER^{T2}CreER^{T2} to enter the nucleus and irreversibly invert the orientation of FlpO (B). FlpO activates expression of both CTIP1 and EGFP, and mice are perfused at P7 (C).
(D-G) In the absence of tamoxifen induction, few electroporated neurons (<5%) recombine the CAG-frt-STOP-frt-EGFP reporter construct (D-D', E-E'), and CTIP1 is expressed at normal levels by neurons in motor cortex (D'', E''). When electroporated pups are dosed with tamoxifen at P2, most electroporated neurons (>95%) recombine the CAG-frt-STOP-frt-EGFP reporter construct (F-F', G-G'), and neurons that have been electroporated with CAG-frt-STOP-frt-CTIP1 express CTIP1 at high levels (G'').
Scale bars: 25µm (all panels).

Figure S6. (related to Figure 6) Thalamocortical axons invade appropriate regions of cortex in the absence of *Ctip1*, and induce appropriate cortical gene expression, despite their failure to organize into sensory maps.
(A-E) Genes regulated in wild-type cortex by thalamocortical innervation, such as *Rorb* (A) and *Cdh8* (C), are expressed in *Ctip1*$^{fl/fl}$*;Emx1-Cre* cortex (B, D), and expression of these genes respects the boundary between motor and sensory cortex (dashed lines in A-D; quantification, E), although sensory maps fail to form.
(F-J) Thalamocortical axons project normally toward the cortical plate at mid-gestation in the absence of *Ctip1* (F, H; insets in G, I). Schematic of experimental approach (J). Quantification in J represents integrated fluorescence intensity of matched areas (boxes in G, I).
(K-L) In wild-type flattened cortex, thalamocortical afferents cluster into a rudimentary sensory map at P1 (K), as revealed by serotonin (5HT) immunostaining. In *Ctip1*$^{fl/fl}$*;Emx1-Cre* flattened cortex, no rudimentary sensory map exists at P1, although sensory thalamocortical axons are appropriately excluded from motor cortex (L).
(M-V) Cholera toxin B (CTB) injected into wild-type and *Ctip1*$^{fl/fl}$*;Emx1-Cre* cortex at P0 retrogradely labels appropriate thalamic nuclei, indicating that thalamocortical axons target appropriate regions of early postnatal cortex. CTB injected into motor cortex (M, O) labels cell bodies in VL (N''', P'''), and CTB injected into somatosensory cortex (M, O) labels cell bodies in VP (N'', P''). CTB injected into visual cortex (Q, S) labels cell bodies in dLG (R''', T'''). Scale bars: 500µm (K, L, M, O, Q, S), 100µm (N, P, R, T).

Figure S7. (related to Figure 7) Layer IV granule neurons express CTIP1, and mosaic deletion of *Ctip1* in layer IV does not disrupt sensory map formation.
(A-C) Most wild-type layer IV granule neurons, labeled by *Scnn1a-Cre*, express CTIP1 at P14 (A-B, quantification in C).
(D-I) Genes normally excluded from layer IV and not expressed by layer IV granule neurons, such as *Gap43* (D), *Nex1* (E), and *Sorl1* (F), are expressed in *Ctip1*$^{fl/fl}$*;Emx1-Cre* layer IV (G-I).
(J-N) Schematic of experimental approach (J). Wild-type or *Ctip1*$^{fl/fl}$ embryos are electroporated at E14.5 with CAG-Cre and CAG-floxed(STOP)-EGFP. Brains with electroporations in S1 are collected at P7 and flatmounted, and tangential sections through layer IV are stained for serotonin (5HT). Electroporated *Ctip1*$^{fl/fl}$ neurons avoid areas of high 5HT expression (M-N), while electroporated wild-type neurons spread across the barrel field (K-L).
(O-Q) Wild-type layer IV neurons electroporated with Cre populate both barrels and septae without apparent discrimination (O), but *Ctip1*$^{fl/fl}$ neurons electroporated with Cre are excluded from barrels (P). Schematic of experimental approach and quantification (Q).
Scale bars: 500µm (K-M), 200µm (A), 100µm (D-I and O-P), 10µm (B).

Figure S8. (related to Figure 8) CTIP1 and COUPTFI are extensively co-expressed in sensory cortex, and each regulates expression of the other.
(A-E) CTIP1 and COUPTFI are co-expressed at low levels in motor cortex, and at higher levels in sensory cortex. Both CTIP1 (A) and COUPTFI (A') are expressed at lower levels in motor cortex (B-B''), and at higher levels in somatosensory cortex (C-C''). Quantification (D-E).
(F-I) In the absence of *Couptf1*, the high levels of CTIP1 expression in wild-type somatosensory cortex (F'') are displaced to the respecified S1 at the caudal aspect of the cortex (G') (M1/S1 boundary, arrows in F, G). In the absence of *Ctip1*, postmitotic expression of COUPTFI is reduced throughout the cortex (H-I), and areally-specified boundaries in COUP-TFI expression are no longer sharp (H'-H''', I'-I''').
Scale bars: 100μm (A), 25μm (B-C), 250μm (F-I).

Table S1. (related to Figure 2) Differential analysis of gene expression between wild-type frontal (M1) and parietal (S1) cortex using RNAseq. Genes differentially expressed between frontal and parietal cortex at P4, reporting reads per kilobase per million reads (RPKM), fold change between frontal and parietal cortex, and p value of differential expression.

Table S2. (related to Figure 2) Differential analysis of gene expression between wild-type parietal and *Ctip1* cKO parietal cortex using RNAseq. Genes differentially expressed between wild-type and *Ctip1* cKO parietal cortex at P4, reporting reads per kilobase per million reads (RPKM), fold change between frontal and parietal cortex, and p value of differential expression.

Table S3. (related to Experimental Procedures) Sequences of plasmids constructed. This table contains sequences for CAG-Cre, CAG-(floxed)STOP-EGFP, CAG-FLEX-Flpo, and CAG-frt-STOP-frt-Ctip1 plasmids.

SUPPLEMENTAL EXPERIMENTAL PROCEDURES

Animals

Unless noted otherwise, all experiments were performed using mice maintained on a C57BL6/J background, and *Ctip1*$^{fl/fl}$*;Emx1-Cre* experimental mice were controlled with *Ctip1*$^{wt/wt}$*;Emx1-Cre*. *Ctip1*$^{fl/fl}$ mice were generated and generously shared by Tucker and colleagues (RRID:MGI_4358088, Sankaran et al., 2009). *Ctip1*$^{-/-}$ mice were generated by Copeland and colleagues (RRID:MGI_2663941, Liu et al., 2003), and were obtained from the RIKEN BioResource Center (stock number RBRC01190). *Bhlhb5-LacZ*, *Lmo4-LacZ,* and *Lmo4*$^{fl/fl}$ mice were generated and generously shared by Gan and colleagues (RRID:MGI_3830526, RRID:MGI_4421422, RRID:MGI_4421414, Deng et al., 2010; Feng et al., 2006). *Couptf1*$^{fl/fl}$ mice were generated and generously shared by Studer and colleagues (RRID:MGI_5523158, Armentano et al., 2007; Tomassy et al., 2010). *Bhlhb5*$^{fl/fl}$ mice were generated by Greenberg and colleagues (RRID:MGI_4440744, Ross et al., 2012), and generously shared by Sarah Ross. *Emx1-Cre* mice were generated by Jones and colleagues (RRID:MGI_4440744, Gorski et al., 2002), and purchased from Jackson Laboratories (stock number 005628). *Scnn1a-Tg3-Cre* and *Rosa26-tdTomato-Ai9* mice were generated by Zeng and colleagues (RRID:MGI_3850187, RRID: MGI_3809523, Madisen et al., 2010), and purchased from Jackson Laboratories (stock numbers 009613 and 007909, respectively). *Gbx2-CreER*^{T2} mice were generated by Li and colleagues (RRID:MGI_3840448, Chen et al., 2009), and purchased from Jackson Laboratories (stock number 022135).

Immunocytochemistry, histology, and *in situ* hybridization

The following primary antibodies and dilutions were used: rabbit anti-5HT, 1:20,000 (ImmunoStar Cat# 20080, RRID:AB_572263); goat anti-BHLHB5, 1:300 (Santa Cruz Biotechnology Cat# sc-6045, RRID:AB_2065343); mouse anti-cleaved caspase 3, 1:500 (Abcam Cat# ab13847, RRID:AB_443014); rabbit anti-COUPTFI, 1:500 (gift from M. Studer; RRID:AB_2566816), mouse anti-CTIP1 clone 14B5, 1:500 (Abcam Cat# ab19487, RRID:AB_444947); rabbit anti-GFP, 1:500 (Molecular Probes Cat# A11122, RRID:AB_221569); goat anti-LMO4, 1:200 (Santa Cruz Biotechnology Cat# sc-11122, RRID:AB_648429); rabbit anti-RORB, 1:1000 (gift from H. Stunnenberg; RRID:AB_2566817). Alexa Fluor-conjugated secondary antibodies (Invitrogen) were used at a dilution of 1:500. For 5HT immunohistochemistry, sections were developed using the Vectastain ABC kit. For cytochrome oxidase staining, 50μm vibratome sections were incubated at 37°C overnight in 0.1M phosphate buffer with 5% sucrose, 0.03% cytochrome *c*, and 0.05% DAB.

***In situ* hybridization probes**

Probe name	Source	Forward primer	Reverse primer
Bhlhe40		gggcagtgatctgatggg	catcagagacggggttgg
Cdh6	Inoue et al., 1997		
Couptf1		aggccagtatgcactcacaaac	agtctctagggagtcagggagc
Crim1	Arlotta et al., 2005		
Crym	Arlotta et al., 2005		
Cux1	Assimacopoulos et al., 2012 (gift of E. Grove)		
Cyp26b1		tctgccccttttgctcttg	acagggatccccttcagc
Dbp		acatctagggacacacccagtc	acatgctaagagcacacacagg
Emx1		ggattcgcacagccttctc	gtgacatcaatgtcctcccc
Emx2		ccgcttatcgaagtccatttag	ccaccatcaccccattaaatac
EphA7		ccggcaggaatatacgagaa	cgaacaccatgaacaccaag
EfnA5		cttttggcaatcctactgttcc	tgctcacttccacactcctaga
Gap43		ggctagcttccgtggaca	aaccggggtacagtgcaa
Grm4		ggtttgaccgatacttctccag	gtcataggggcaggtcttacag
Id2		ctggactcgcatcccact	ggctcgtgtcaaaaaggc
Kitl	Cederquist et al., 2013		
Lmo4	Joshi et al., 2005		
Mdga1		gttgcaaagatgatgagagctg	tggctgatcagagtcaggtaga
Nex1		gtccttcgaggaaagagcatta	caaggtttcttcttgcttcagg
Odz3		cgctcaccaaactaatccactt	gaagtgcaggttctccaggtag
Pax6		gggagtgcccttccatct	cccatgggctgactgttc
Rorb		tgcaacattaggaatgtcctgc	acagcaaatcacatgaaagcc
Sert		ccatcagtcctctgtttctcct	ggacagacacaagagctcacac
Sorl1		ggttggagagagcatatggaag	ttagggtttcggtagaggtcaa

Quantitative PCR

Rostral/caudal or medial/lateral pieces of whole cortex were dissected from E15.5 wild-type embryos (n=4 of each set), and cDNA was prepared from extracted RNA using Superscript III reverse transcriptase (Life Technologies). qPCR was performed using Taqman probes (*Ctip1*: Mm00479358; *Nex1*: Mm01326464; *Actb*: Mm00607939) on a StepOnePlus thermal cycler (Life Technologies).

Cortical flattening

Mice were transcardially perfused with 4% paraformaldehyde, and brains were dissected and cut along the midline. Subcortical, midbrain, and hippocampal structures were dissected away under a dissecting microscope, leaving a hollow hemisphere of cortex. Cortex was flattened between glass slides with 1.1mm spacers and post-fixed overnight with 4% paraformaldehyde at 4°C.

Anterograde labeling with AAV

Neurons were labeled by pressure injection of virus under ultrasound guidance at P1, and brains were collected at P7. For quantification, matched thalamic sections (Figure 4) or matched cortical sections (Figure S3 and 7) (n=3 mice for each genotype) were imaged, and fluorescence intensity was measured across images using ImageJ

The pAAV-EGFP construct was obtained from the MGH Virus Core and contains the following elements flanked by AAV2 ITRs: a CMV/β-actin promoter, the coding sequence for EGFP, the woodchuck hepatitis virus post-transcriptional regulatory element (WPRE), a bovine GH pA signal, and an SV40 pA signal (full sequence available upon request). The pAAV-tdTomato construct was generated by replacing the EGFP coding sequence in pAAV-EGFP with the coding sequence for tdTomato obtained from pTdTomatoN1 (Clonetech). Both constructs were packaged and serotyped with the AAV2/1 capsid protein by the MGH Virus Core.

Quantification of callosal connectivity

Matched coronal sections from wild-type and *Ctip1*$^{fl/fl}$ brains (n=3 mice for each genotype), all with comparable electroporations, were imaged for EGFP on both the electroporated and the contralateral sides. In order to quantify fluorescence across the entire mediolateral extent of cortex, the straighten plug-in for ImageJ (Kocsis et al., 1991) was used to gather a 400um (200 pixel) radial swath of cortex extending from the M1/S1FL border to the InsCx/PirCx border. The resulting rectangular image (200 pixels high by 2000 pixels wide) was binned into 200 segments (200 pixels high by 10 pixels wide), and fluorescence intensity in each bin was quantified. A plot of normalized average fluorescence intensity (and standard error of the mean) against mediolateral position across three brains was generated. Fluorescence intensity was also quantified by cortical area (M1/M2, S1FL, S1J, S1ULp, S2, and InsCx), and the difference between means for wild-type and *Ctip1*$^{fl/fl}$ brains was analyzed using an unpaired Student's t-test.

Retrograde labeling

CSMN were labeled from their axonal projections in the spinal cord at P21 by pressure injection (Nanoject II, Drummond) of ~240nl of Alexa Fluor-conjugated cholera toxin B (CTB) (Invitrogen) into the dorsal corticospinal tract between C1 and C2. Brains were collected three days later. For quantification, four adjacent sections from anatomically-matched rostrocaudal positions were counted from each mouse (n=3 mice for each genotype) by investigators blinded to genotype. Thalamocortical neurons were labeled from their axonal projections in the cortex at P0 by pressure injection of ~80nl of Alexa Fluor-conjugated CTB into appropriate cortical areas. Brains were collected on the following day.

Subcerebral projection neurons were labeled from the cerebral peduncle under ultrasound guidance (Vevo 770) at P1 by pressure injection of Alexa fluorophore-conjugated cholera toxin B (Invitrogen). Brains were collected at P4.

***In utero* electroporation**

Briefly, plasmids were microinjected into the lateral ventricle of developing embryos under ultrasound guidance, and electroporated into cortical progenitors using a square wave electroporator (CUY21EDIT, Nepa Gene, Japan), set to deliver five 30V pulses of 50ms, separated by 950ms intervals. Tamoxifen induction was accomplished by intraperitoneal injection of 4OH-tamoxifen dissolved in corn oil (100ul at 5mg/ml; Sigma-Aldrich H6278 and C8267).

Figure	**Genotype**	**Plasmids**	**Age (ep)**	**Age (recovery)**
2	*Ctip1*$^{wt/wt}$ (control) *Ctip1*$^{fl/fl}$ (experimental)	CAG-*Cre* CAG-floxed(STOP)-*Egfp*	E14.5	P7
5	Wild-type	CAG-*CreER*^{T2} CAG-FLEX-*Flpo* CAG-frt-STOP-frt-*Egfp* CAG-frt-STOP-frt-*Ctip1* (experimental)	E12.5	P21
7	*Ctip1*$^{wt/wt}$ (control) *Ctip1*$^{fl/fl}$ (experimental)	CAG-*Cre* CAG-floxed(STOP)-*Egfp*	E14.5	P7
8	*Ctip1*$^{fl/fl}$*;Emx1-Cre*	CAG-floxed(STOP)-*Egfp* CAG-floxed(STOP)-*Ctip1* (experimental)	E14.5	P7
S7	*Ctip1*$^{wt/wt}$ (control) *Ctip1*$^{fl/fl}$ (experimental)	CAG-*Cre* CAG-floxed(STOP)-*Egfp*	E14.5	P7
S7	*Ctip1*$^{wt/wt}$ (control) *Ctip1*$^{fl/fl}$ (experimental)	CAG-*Cre* CAG-floxed(STOP)-*Egfp*	E13.5	P7

CMV/β-actin promoter-driven *Cre*, floxed(STOP)-*Egfp*, FLEX-*FlpO*, ER^{T2}CreER^{T2}, and frt-STOP-frt-*Ctip1* plasmids were derived from CBIG, gift of C. Lois. ER^{T2}CreER^{T2} was subcloned from pCAG-ER^{T2}CreER^{T2} (Addgene plasmid 13777) and frt-STOP-frt was subcloned from pCAFNF-*Egfp* (Addgene plasmid 13772).

For tamoxifen-inducible Cre electroporations, highly efficient recombination upon tamoxifen induction was accomplished by using a FLEX-*FlpO* construct to couple relatively inefficient recombination by *ER^{T2}-Cre-ER^{T2}* with robust recombination of *frt-STOP-frt* cassettes by constitutively active *Flp* recombinase (Figure S5D-G). Expression constructs for *ER^{T2}-Cre-ER^{T2}* and FLEX-*FlpO*, together with conditional expression constructs for *EGFP* and/or *Ctip1*, were electroporated into the cortical ventricular zone at E12.5, and the resulting pups were injected with tamoxifen at P2 (Figure 5A-5C).

Sequences

See Table S3.

SUPPLEMENTAL REFERENCES

Chen, L., Guo, Q., Li, J. Y. H, 2009. Transcription factor Gbx2 acts cell-nonautonomously to regulate the formation of lineage-restriction boundaries of the thalamus. Development 136, 1317-1326. doi:10.1242/dev.030510

Gorski, J.A., Talley, T., Qiu, M., Puelles, L., Rubenstein, J.L.R., Jones, K.R., 2002. Cortical excitatory neurons and glia, but not GABAergic neurons, are produced in the Emx1-expressing lineage. J Neurosci 22, 6309–6314. doi:20026564

Kocsis, E., Trus, B.L., Steer, C.J., Bisher, M.E., and Steven, A.C. (1991). Image averaging of flexible fibrous macromolecules: the clathrin triskelion has an elastic proximal segment. J. Struct. Biol. 107, 6–14.

Madisen, L., Zwingman, T.A., Sunkin, S.M., Oh, S.W., Zariwala, H.A., Gu, H., Ng, L.L., Palmiter, R.D., Hawrylycz, M.J., Jones, A.R., Lein, E.S., Zeng, H., 2010. A robust and high-throughput Cre reporting and characterization system for the whole mouse brain. Nat Neurosci 13, 133–140. doi:10.1038/nn.2467

Tomassy, G.S., De Leonibus, E., Jabaudon, D., Lodato, S., Alfano, C., Mele, A., Macklis, J.D., Studer, M., 2010. Area-specific temporal control of corticospinal motor neuron differentiation by COUP-TFI. Proceedings of the National Academy of Sciences 107, 3576–3581. doi:10.1073/pnas.0911792107